BERLIN 1987

ETA FACTORS, FAILURE ASSESSMENT DIAGRAMS AND VALIDITY FOR CONVENTIONAL AND NOVEL SPECIMEN GEOMETRIES : SOME RESULTS FROM THEORY AND EXPERIMENT

R Bradford, R Gates, G Green, D Gladwin, J Buckland, A Muscati
CEGB SW Region

SUMMARY

Results are summarised for 4 specimen geometries for which theoretical and experimental investigations have been made. In many cases comparisons are possible, which provide checks on the theoretical or empirical techniques used. The analyses were originally performed for a variety of reasons. The Failure Assessment Diagrams were derived as one of the many inputs to the new Revision 3 to the R6 procedure. In one case, FE analysis was performed to investigate the validity of Mode II toughnesses derived from a novel specimen and being used to assess existing structures. Perhaps the most useful outcome of theoretical analyses is the derivation of eta factors which allow experimental estimation of J from a single load-displacement record. This is most important for novel geometries or where strain hardening causes deviations from the 'classical' (perfectly-plastic) value.

Theoretical Analysis is an important adjunct to experimental techniques in the following cases:

Eta Factors

Frequently experimentalists wish to find J from a single load-displacement record. A theoretical calculation of the constant (η) relating to J to U is therefore required.

$$J = \eta \frac{U\ (\text{TOTAL})}{\text{Ligament Area}}$$

Validity

Direct verification of the validity of applying small specimen toughness measurements to large structures is problematical due to the difficulty of testing large structures (and expense!). Theoretical investigations based on the occurrence of universal crack tip fields (HRR) are therefore important.

Failure Assessment Diagrams

As well as giving the elastic solution (K), theoretical analysis is important as an independent source of FAD's. This is particularly true in the crucial "knee" region (elastic-plastic transition) where experimental errors are greatest. Finite element analysis provides a convenient means of investigating the effect on the FAD of changing a single factor, eg. stress/strain curve or specimen geometry.

(1) Elastic-plastic finite element analysis is a good method of deriving eta factors, enabling J to be found simply from a load-displacement record.

(2) Extensive investigations for the CCP show good agreement in η between theoretical and experimental methods, confirming the effect of strain hardening.

(3) In plane stress, the CCP and DPS are both apparently valid well beyond general yield (HRR fields), and this is consistent with experimental evidence on initiation toughness.

(4) Plateaux can occur in specimen load-displacement curves due to Luders behaviour or a plane strain/plane stress transition. The CCP analysis has confirmed that including the plateau area in estimating J is correct, and that this J controls the crack tip fields.

(5) The geometry dependence of the derived failure assessment diagram is slight, especially when compared with typical uncertainties in theoretical estimates of the normalising load (yield load or flow load).

(6) The finite element method, the experimental method, and the reference stress method (Option 2 of R6) give broadly consistent FAD's when variations in the stress-strain data or geometry are considered.

(7) Empirical yield and collapse loads can depend upon 3D effects (plane strain/plane stress transition and geometry change) so that theoretical estimates based on 2D infinitesimal strain theory are necessarily simplistic.

(8) The end point of stable tearing, in both Modes I and II, is unstable tearing (ductile fracture), as distinct from collapse of the remaining ligament.

(1) Elastic-plastic finite element analysis is a good method of deriving eta factors, enabling J to be found simply from a load-displacement record.

(2) Extensive investigations for the CCP show good agreement in η between theoretical and experimental methods, confirming the effect of strain hardening.

(3) In plane stress, the [redacted] DPS is [redacted] apparently valid well beyond general yield (HRR fields), and this is consistent with experimental evidence on initiation toughness. CCP ?

(4) Plateaux can occur in specimen load-displacement curves due to Luders behaviour or a plane strain/plane stress transition. The CCP analysis has confirmed that including the plateau area in estimating J is correct, and that this J controls the crack tip fields.

(5) The geometry dependence of the derived failure assessment diagram is slight, especially when compared with typical uncertainties in theoretical estimates of the normalising load (yield load or flow load).

(6) The finite element method, the experimental method, and the reference stress method (Option 2 of R6) give broadly consistent FAD's when variations in the stress-strain data or geometry are considered.

(7) Empirical yield and collapse loads can depend upon 3D effects (plane strain/plane stress transition and geometry change) so that theoretical estimates based on 2D infinitesimal strain theory are necessarily simplistic.

(8) The end point of stable tearing, in both Modes I and II, is unstable tearing (ductile fracture), as distinct from collapse of the remaining ligament.

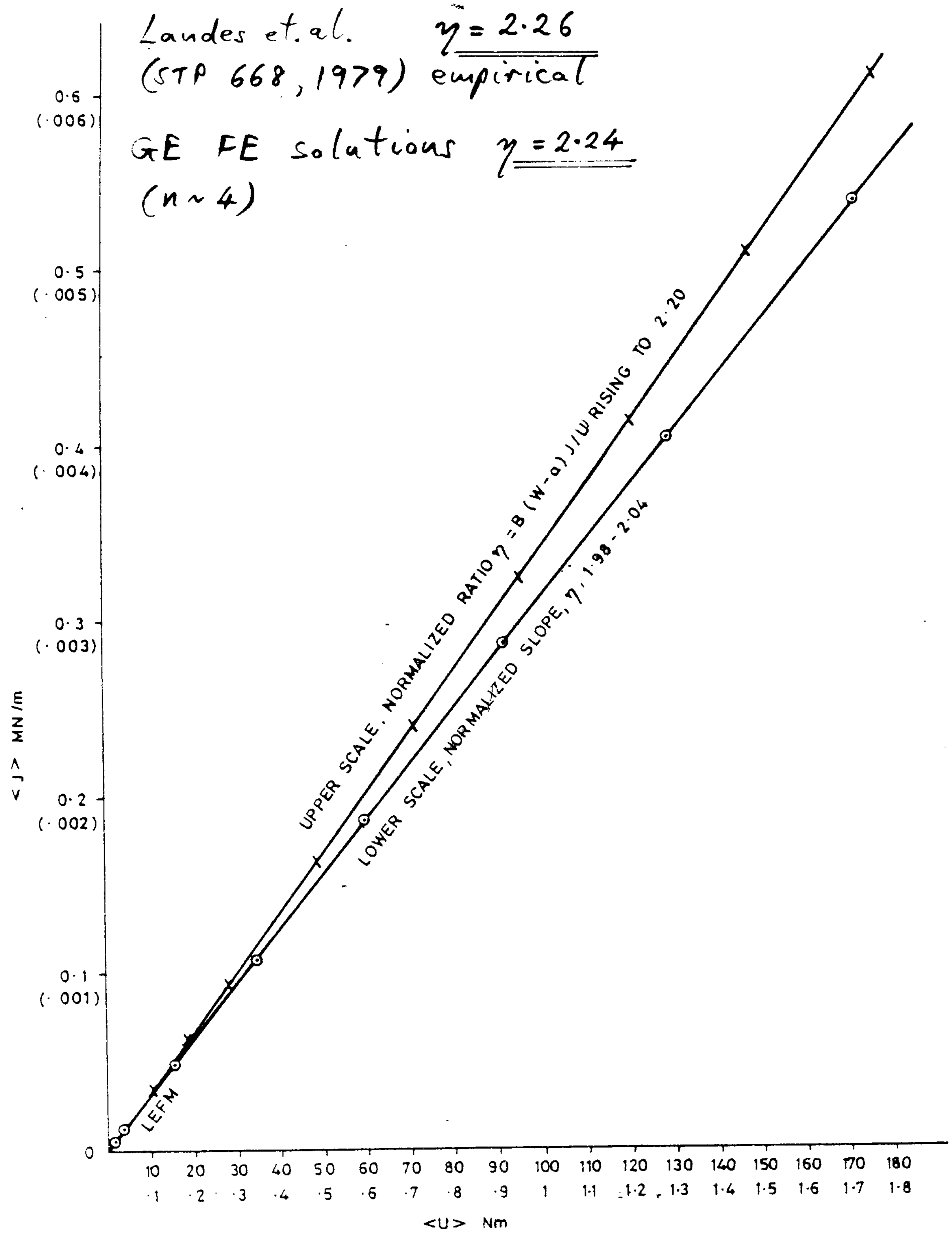

FIG. 1. J VERSUS ENERGY <U> A/W = 0.5

Finite Elements CTS

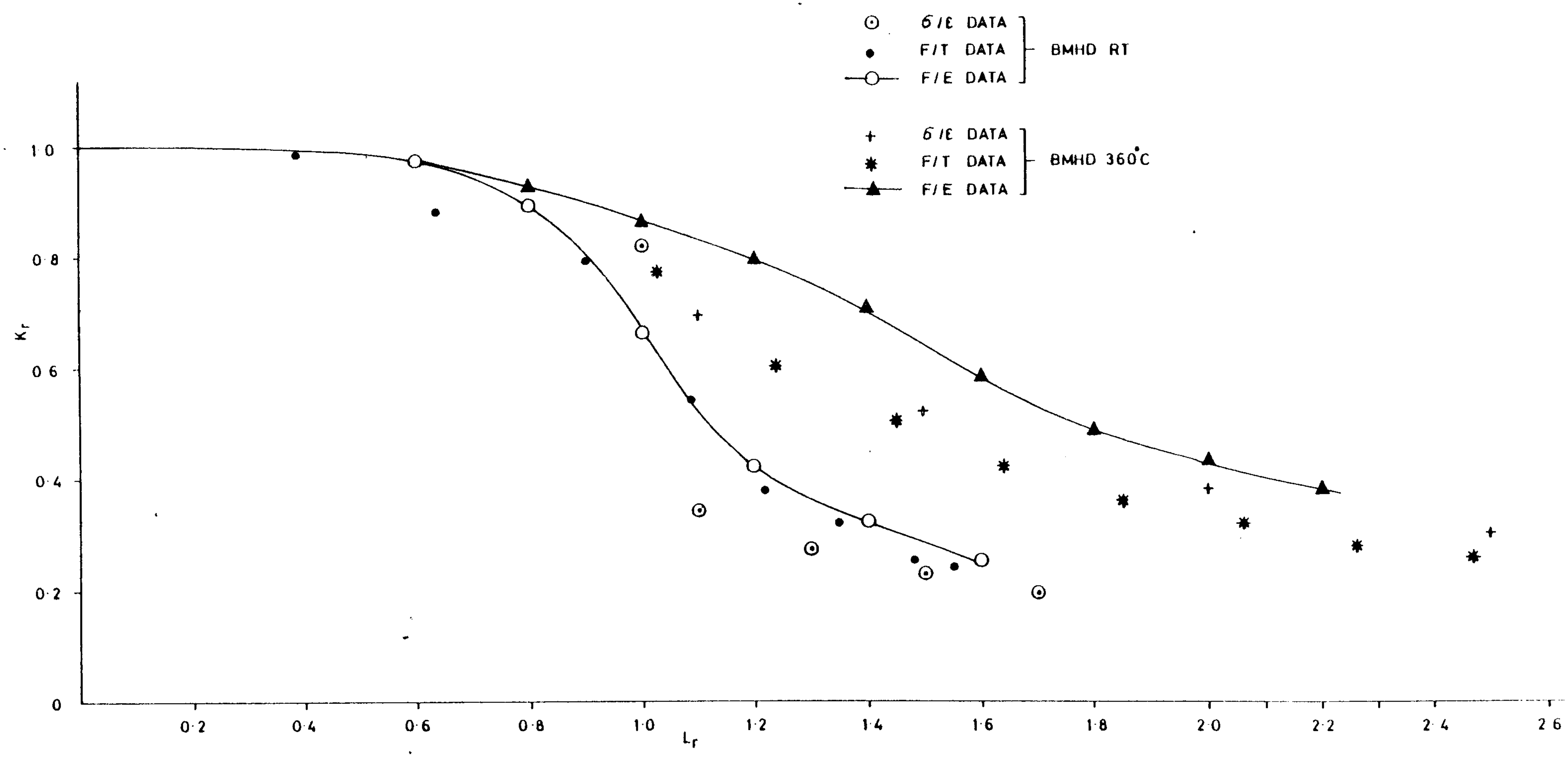

FIG. 2. COMPARISON OF FAD's DERIVED FOR C/Mn STEEL. CTS

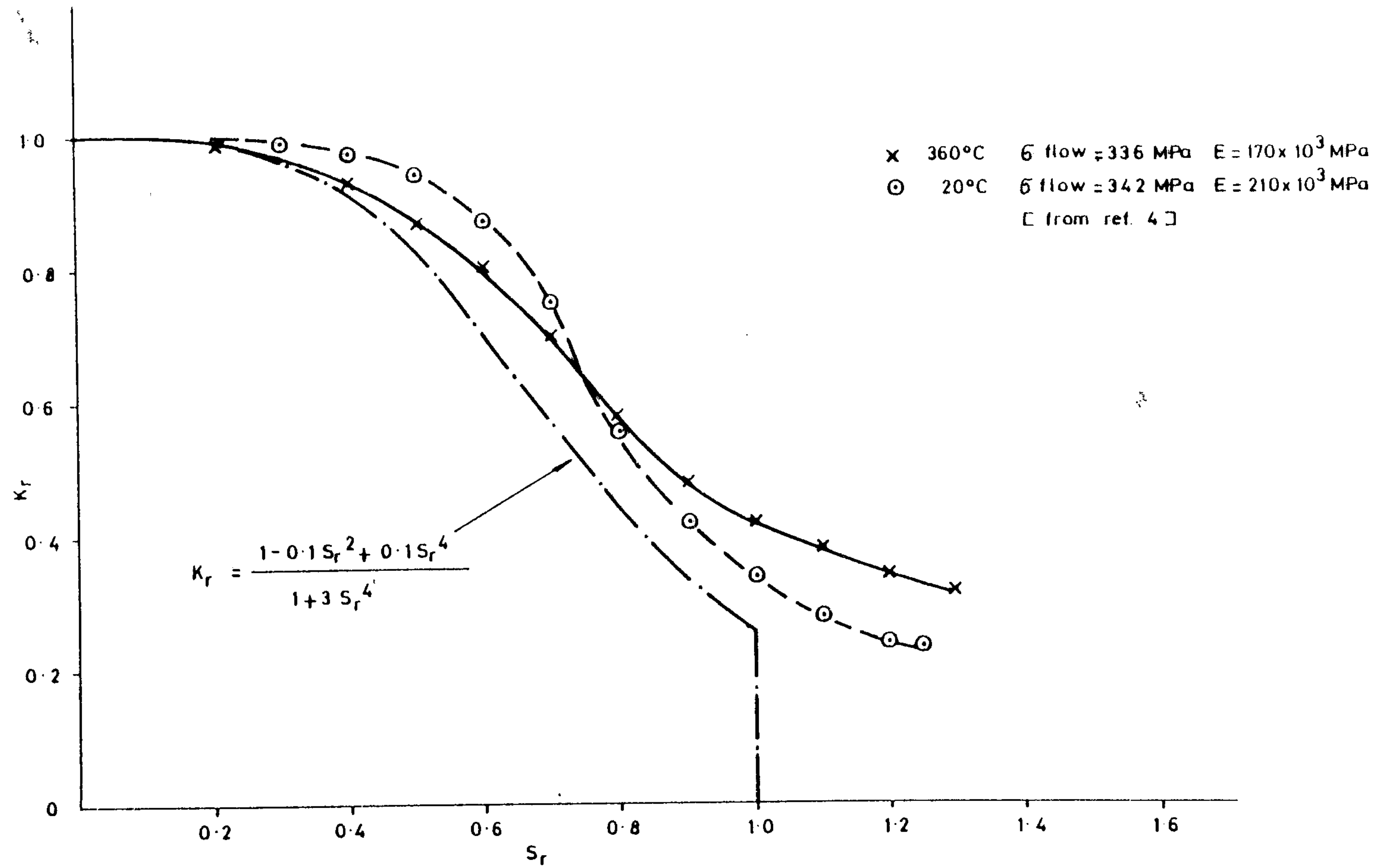

FIG. 3. FAILURE ASSESSMENT DIAGRAM DERIVED FROM FINITE ELEMENT CALCULATIONS.

CTS

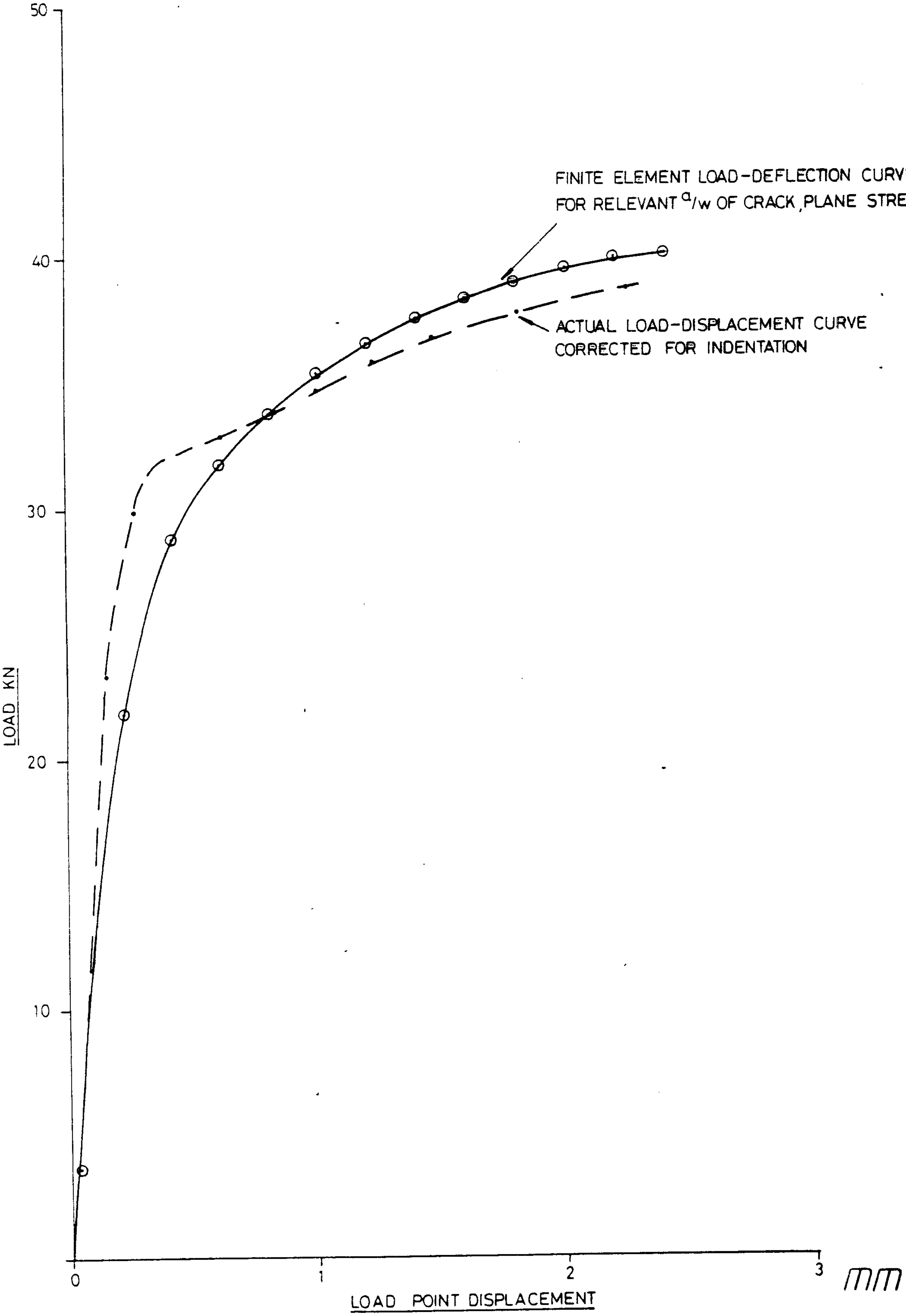

SSD/SW/R417

FIG 4 COMPARISON OF ACTUAL AND CALCULATED LOAD-DISPLACEMENT CURVE FOR A/W = •514 CTS

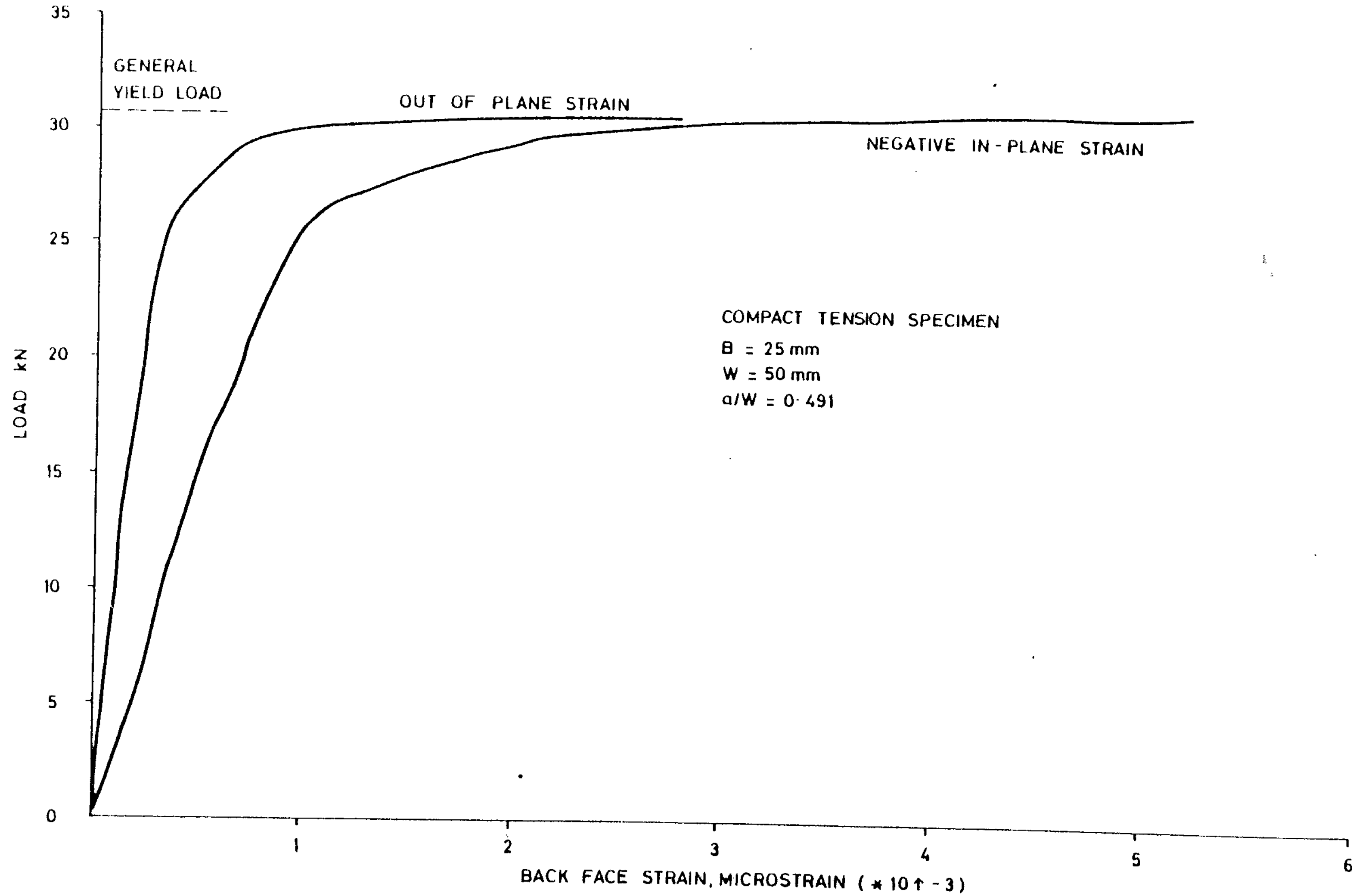

FIG. 5. BACK FACE STRAIN/LOAD TEST RECORD.

CTS

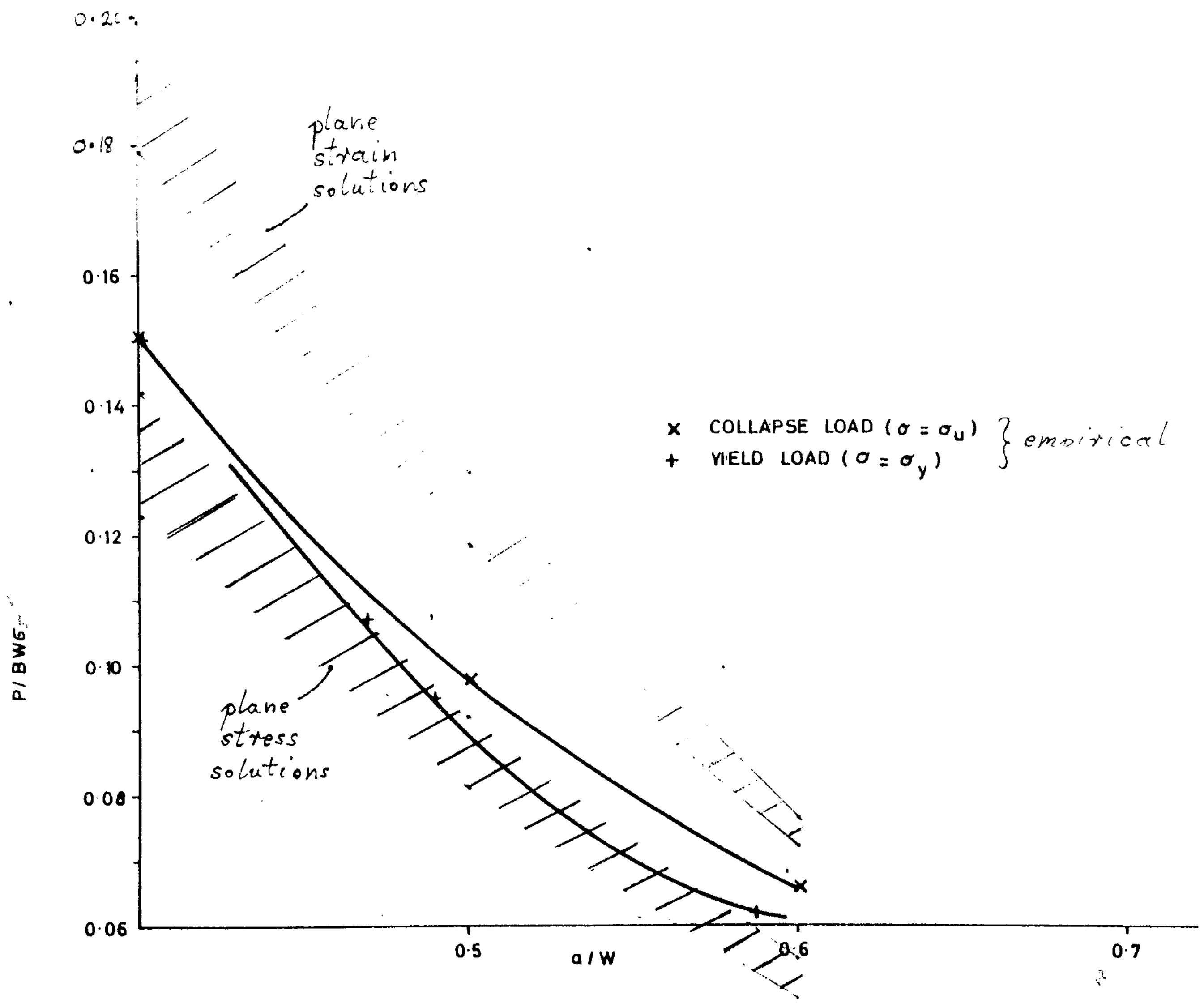

FIG. 6. VARIATION OF NORMALISED YIELD AND COLLAPSE LOADS WITH CRACK LENGTH FOR COMPACT TENSION SPECIMENS.

Comparison of Experiment with Theoretical Solutions in Plane Stress and Plane Strain

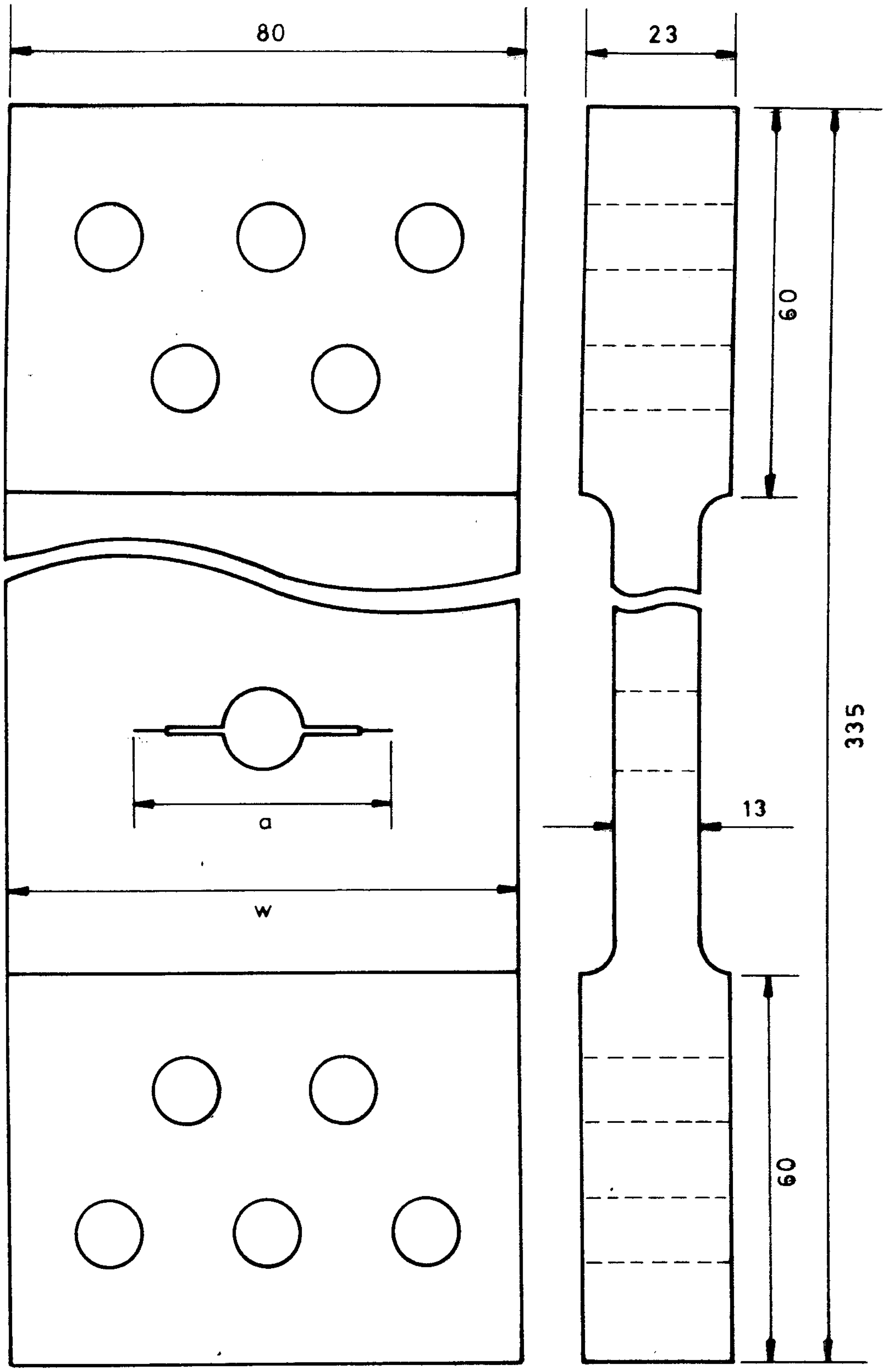

ALL DIMENSIONS IN mm

FIGURE 7 CENTRE CRACKED PANEL SPECIMEN GEOMETRY

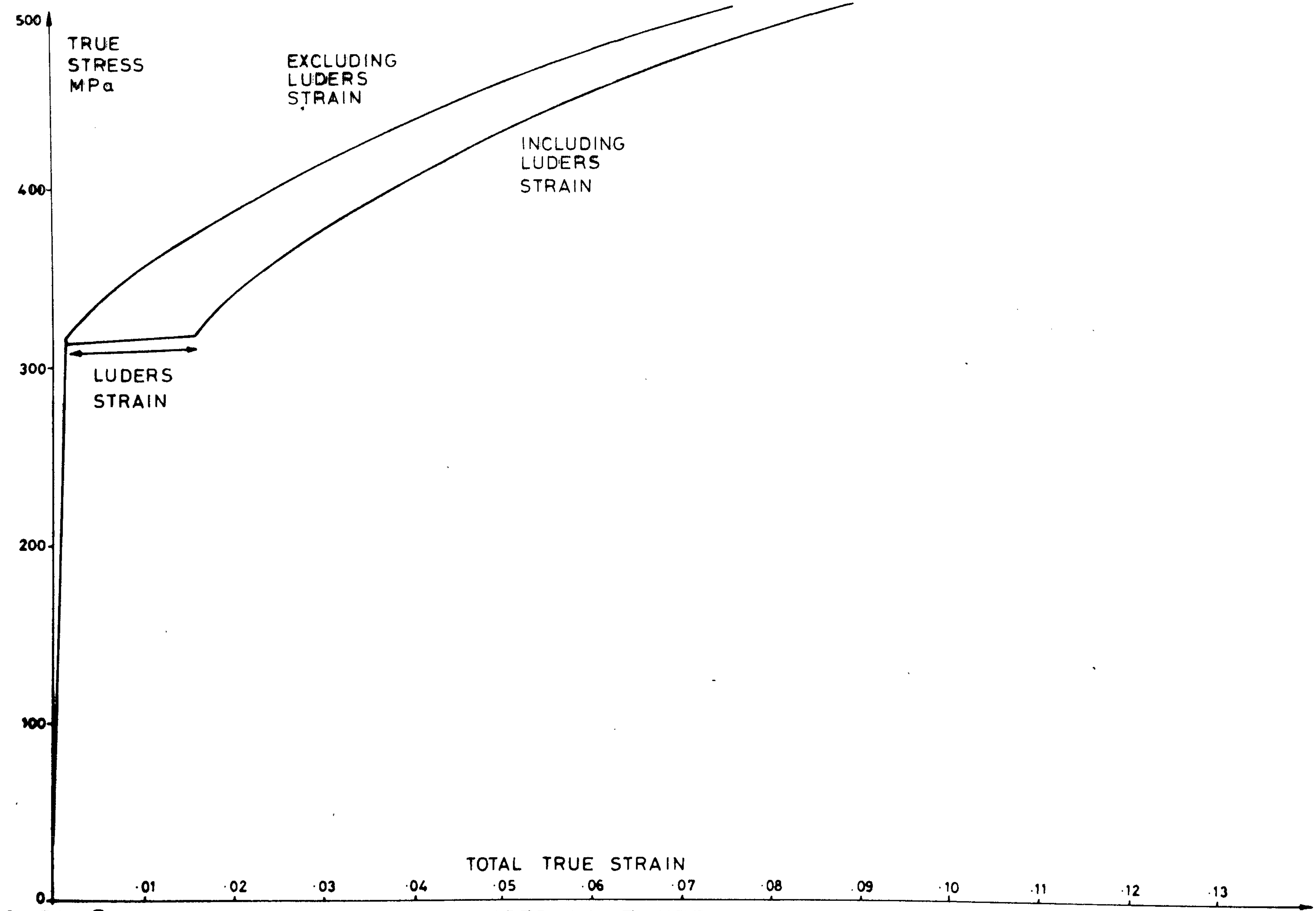

FIGURE 8 STRESS-STRAIN DATA USED IN FINITE ELEMENT ANALYSIS *OF CCP*

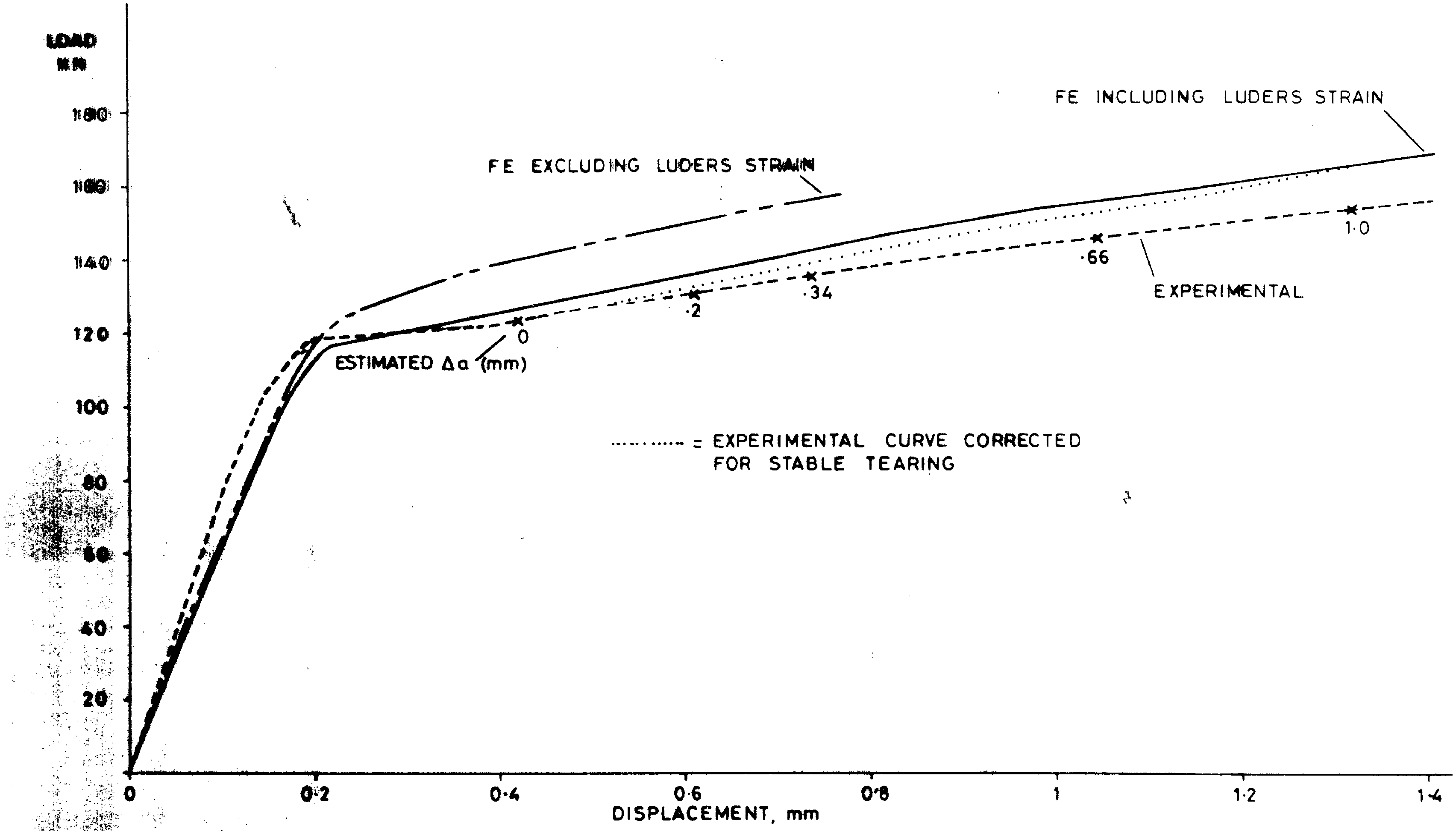

FIG. 9 LOAD DISPLACEMENT CURVES : COMPARISON OF EXPERIMENTAL AND FINITE ELEMENT RESULTS CCP, a/w = 0·65

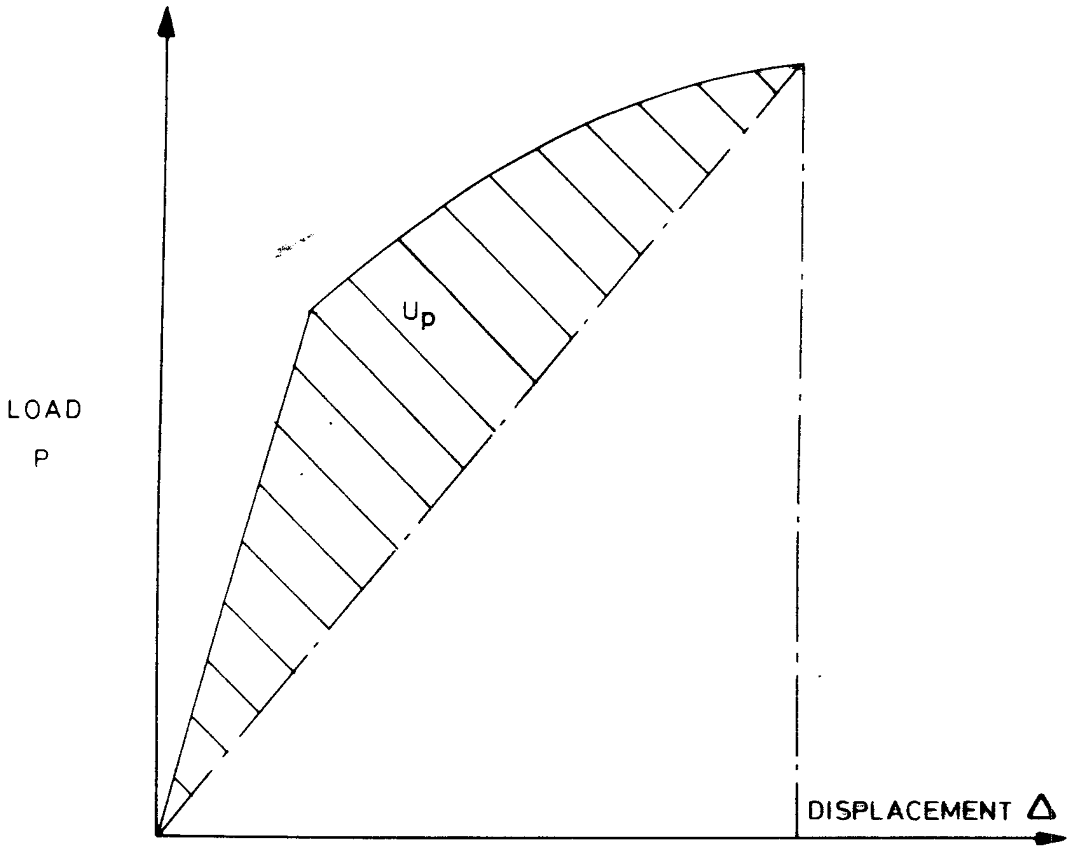

RICE PARIS AND MERKLE METHOD (STP 536, ASTM 1973)

$$J = J_{(elastic)} + \frac{2\,U_p}{A_{(ligament)}}$$

Defining η such that $J = \eta \dfrac{U_{(TOTAL)}}{A_{ligament}}$

RPM formula implies $\eta < 1$ in far plastic regime.

For power-law hardening, $\varepsilon \propto \sigma^n$ we get

$$\eta = 1 - \frac{1}{n}$$

Fig. 10 Simple Theory Prediction for Eta Factor of Tension Geometry (CCP)

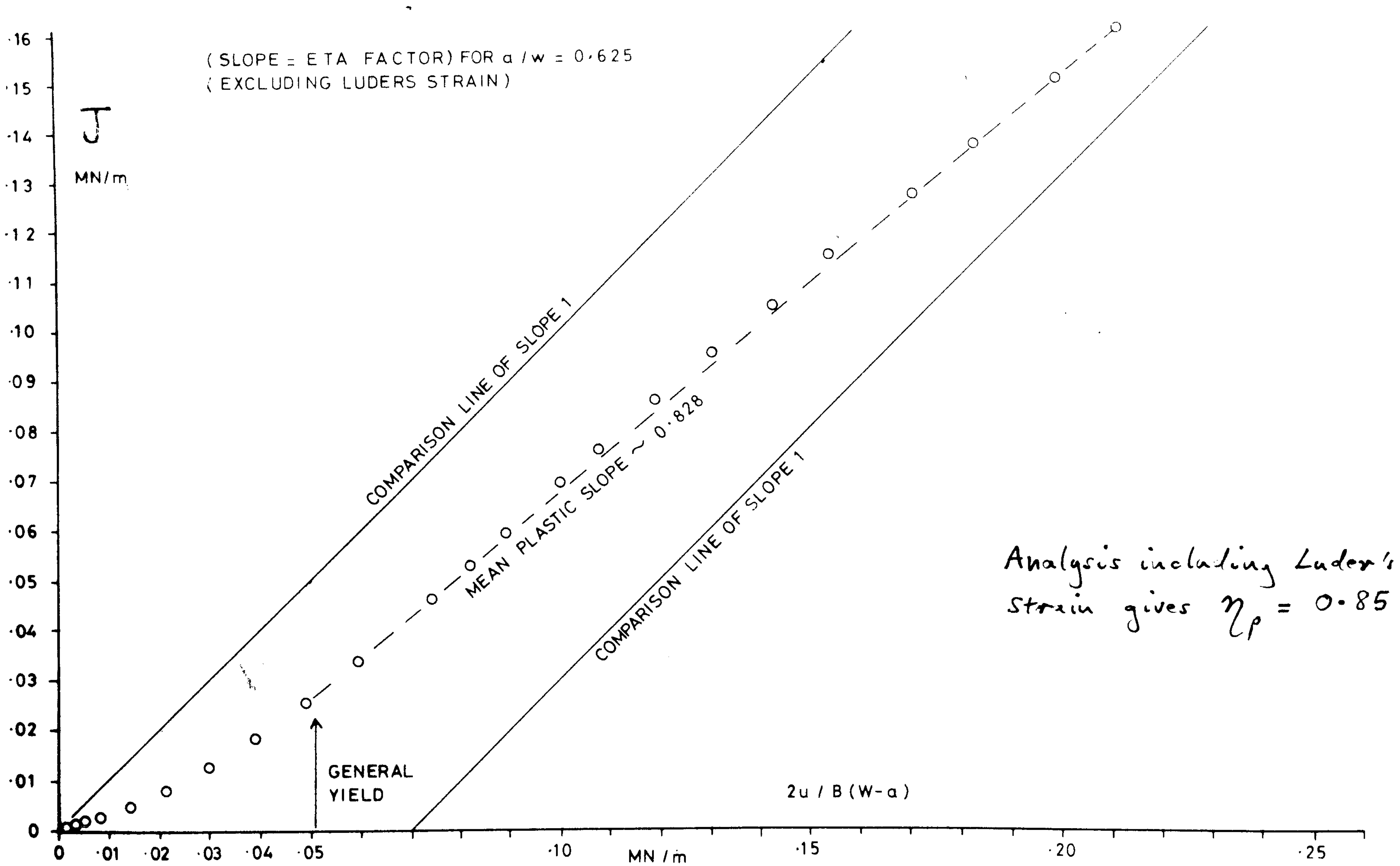

FIG. 11 ELASTIC PLASTIC J VERSES NORMALIZED ENERGY CCP

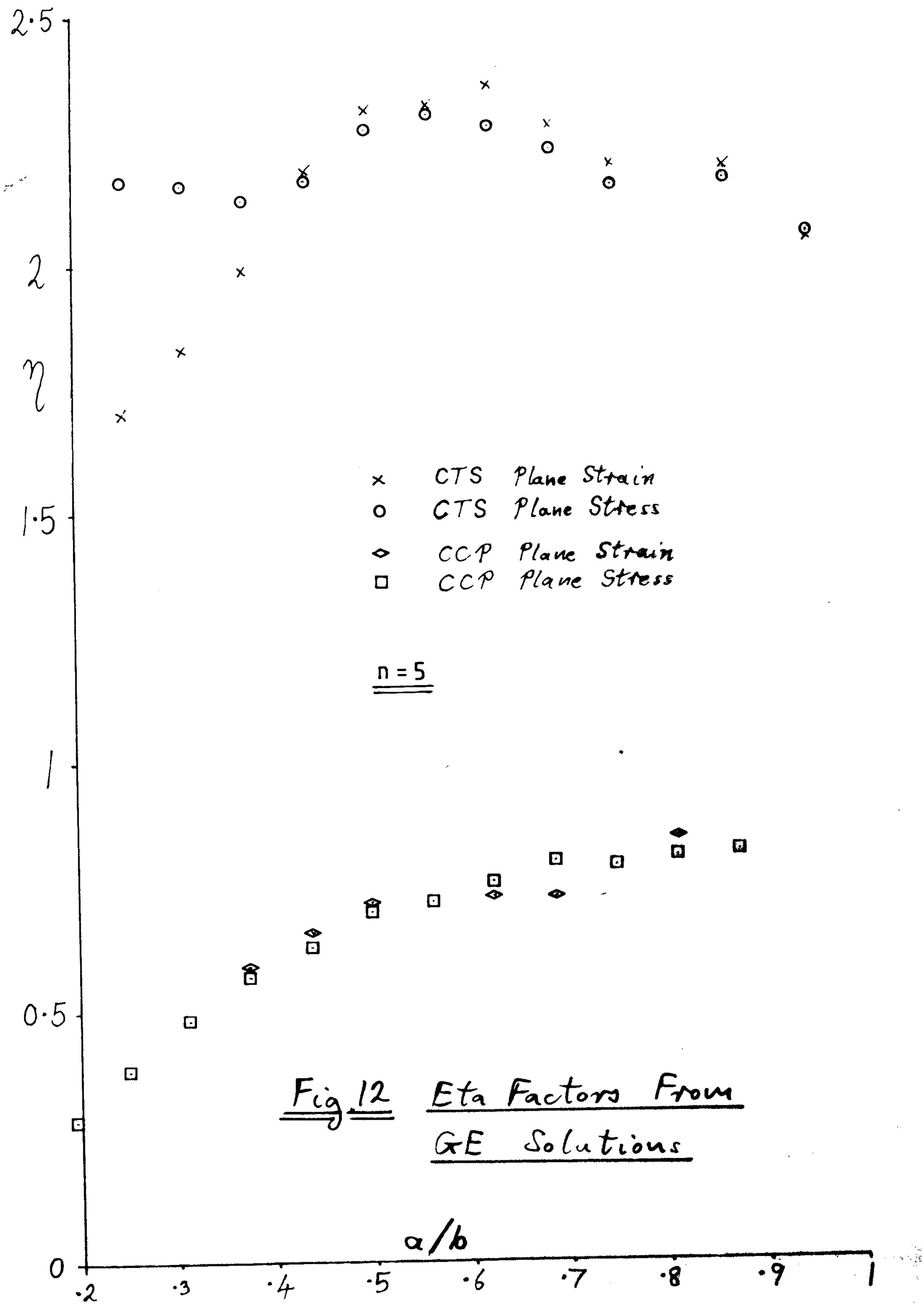

Fig 12 Eta Factors From GE Solutions

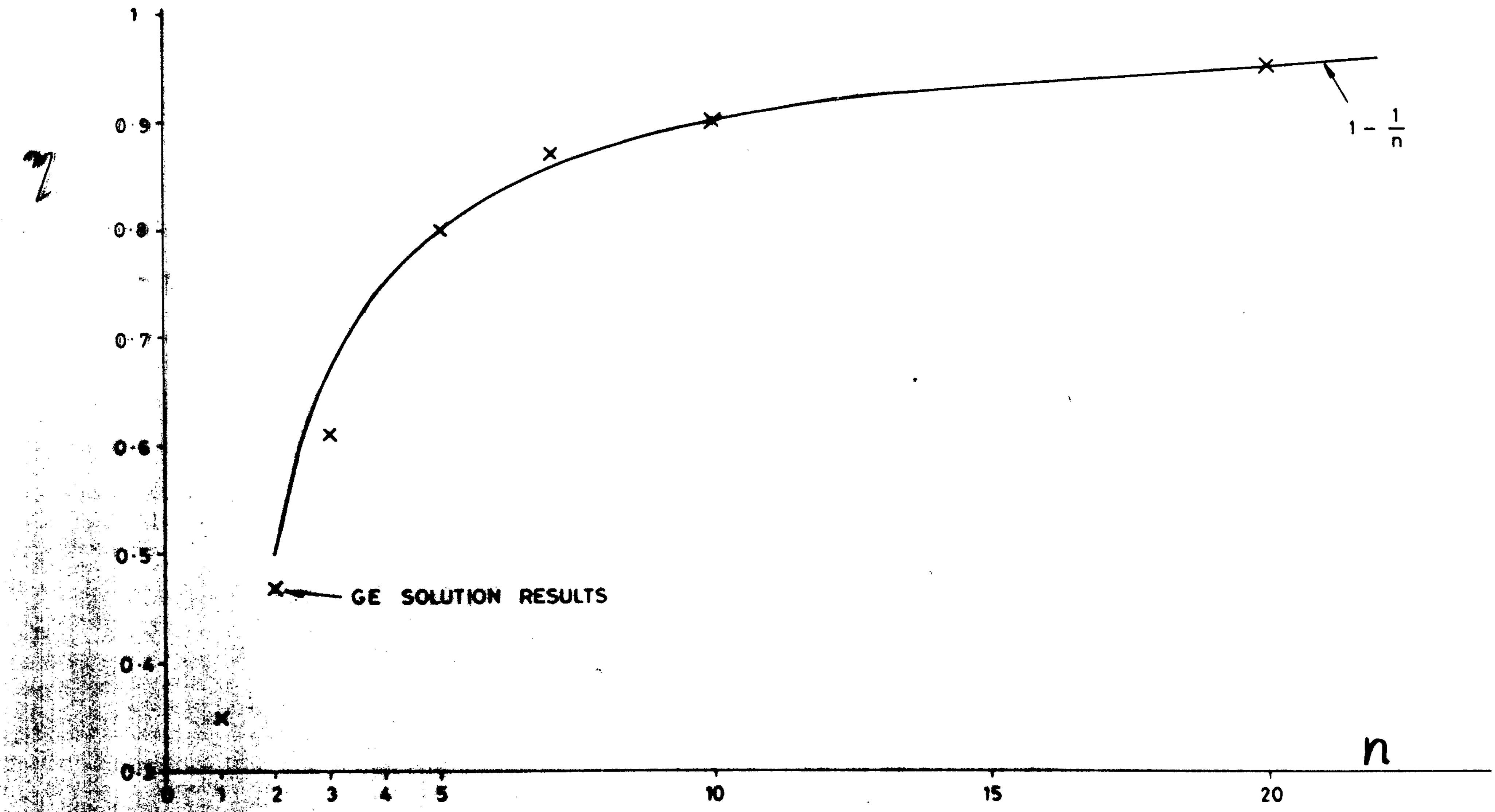

FIG. 13 SIMPLE THEORY V. GE SOLUTION (HARDENING DEPENDENCE)
CCP PLANE STRESS a/b = 0·69

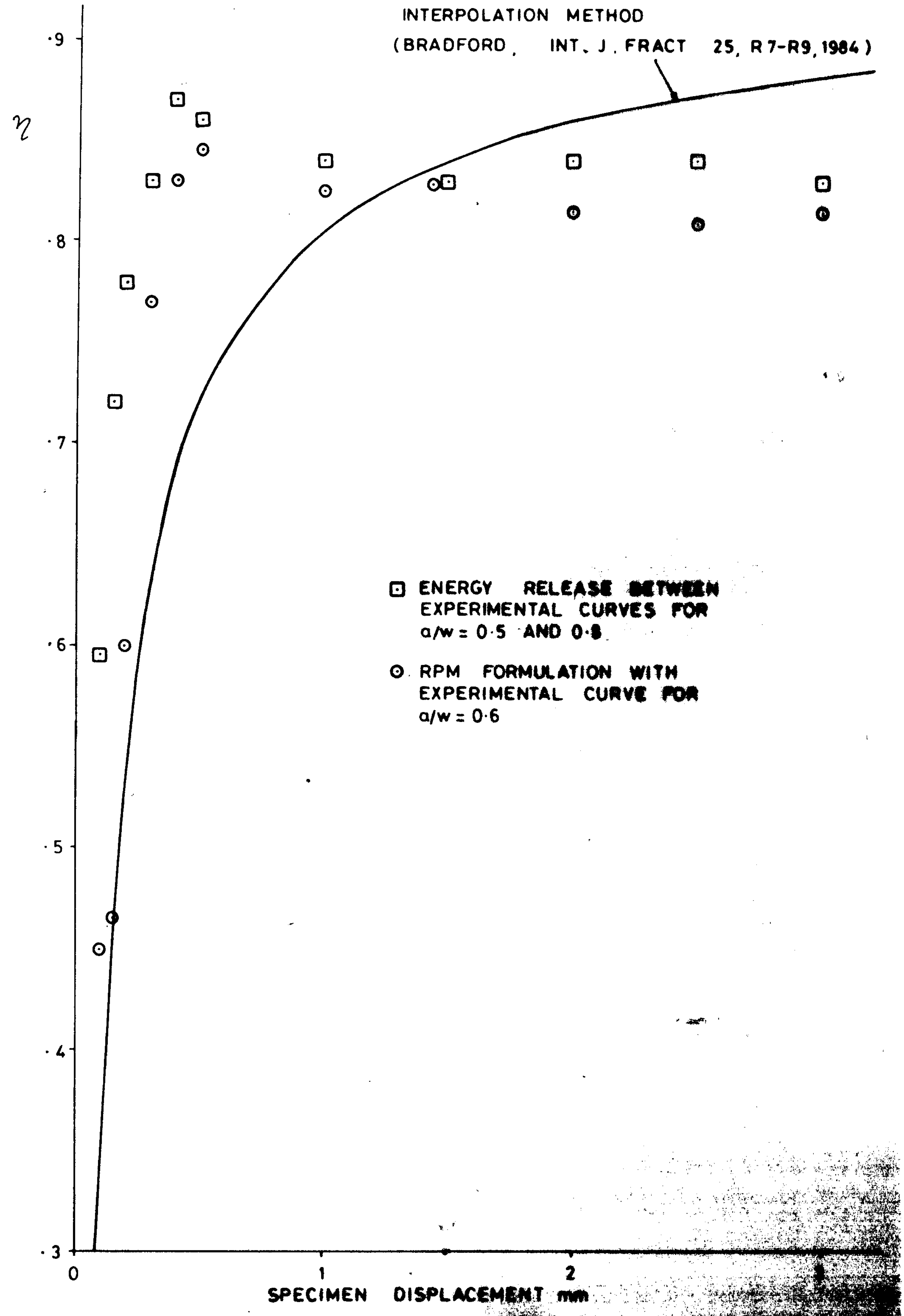

FIG. 14 EMPIRICAL γ - ESTIMATES CCP (a/w

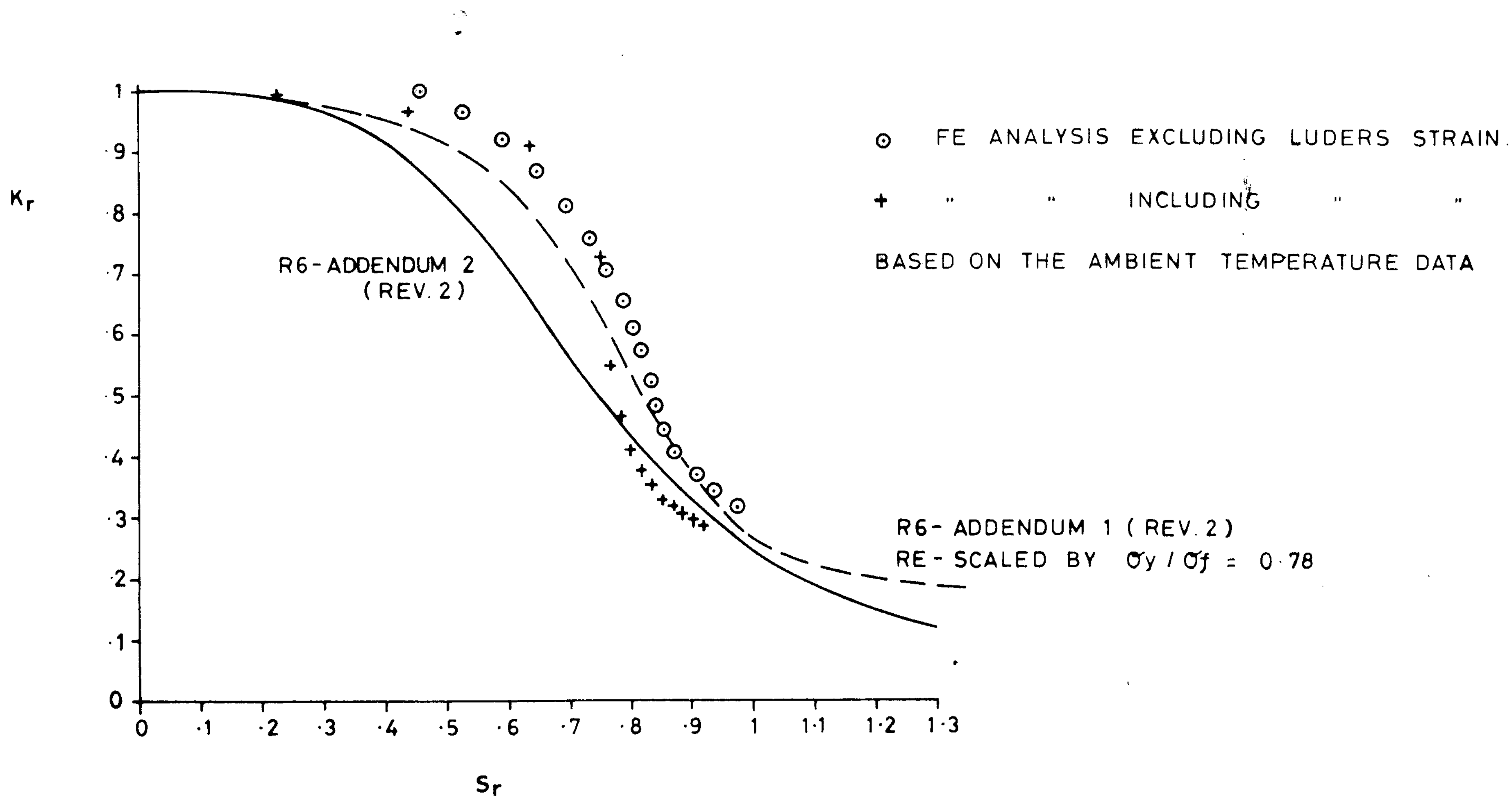

FIGURE 15 COMPARISON OF FAD'S FROM FE ANALYSIS AND R6 ("OPTION 1")

CCP

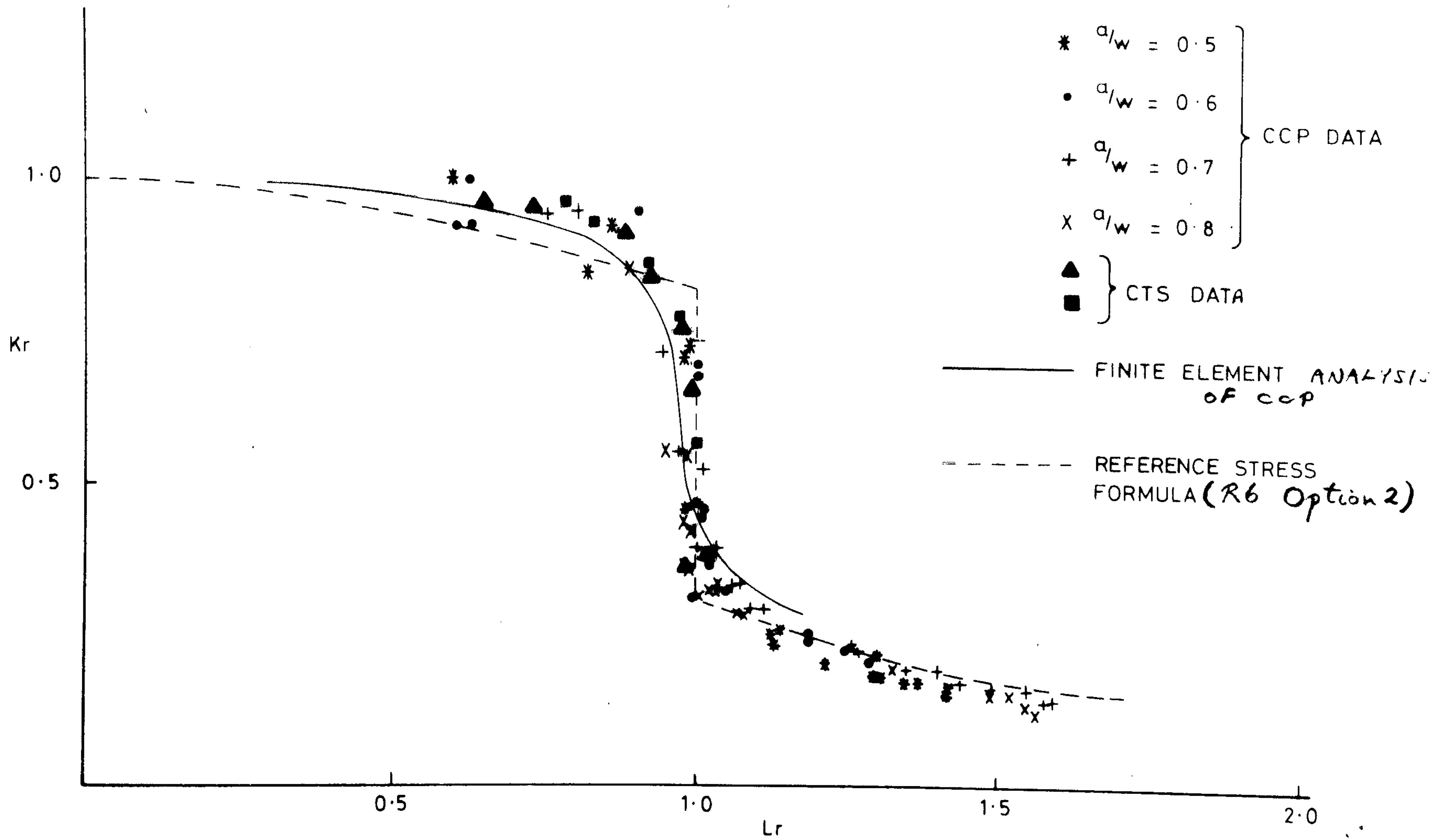

FIG. 1·7 COMPARISON OF EXPERIMENTAL FAILURE ASSESSMENT DIAGRAMS & DIAGRAMS DERIVED BY INCLUDING THE LUDERS STRAIN & USING FE ANALYSIS OR THE REFERENCE STRESS FORMULA

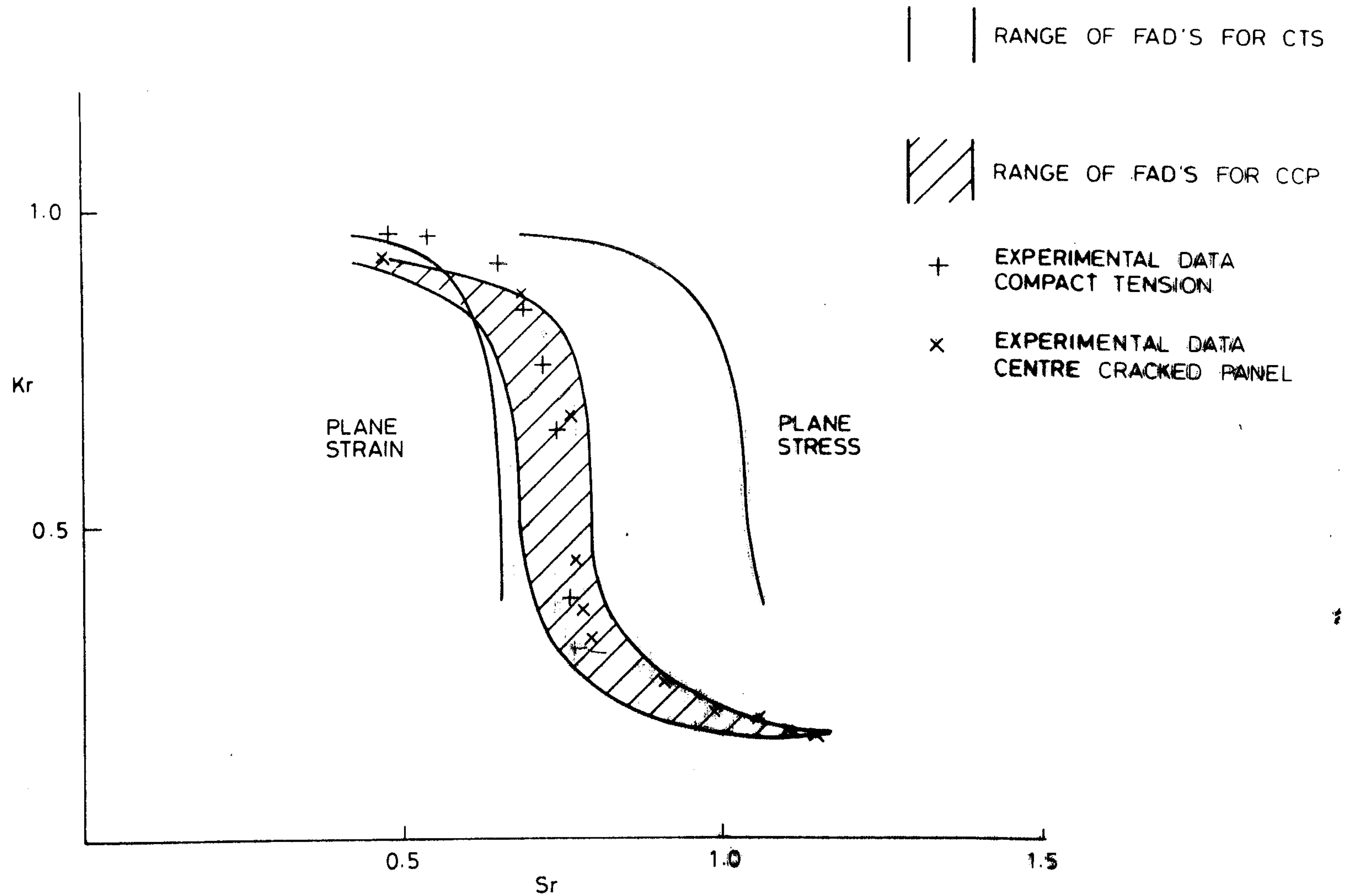

FIG. 18 EFFECTS OF CHOICE OF LOAD NORMALISATION PARAMETER ON FAILURE ASSESSMENT DIAGRAM POSITION

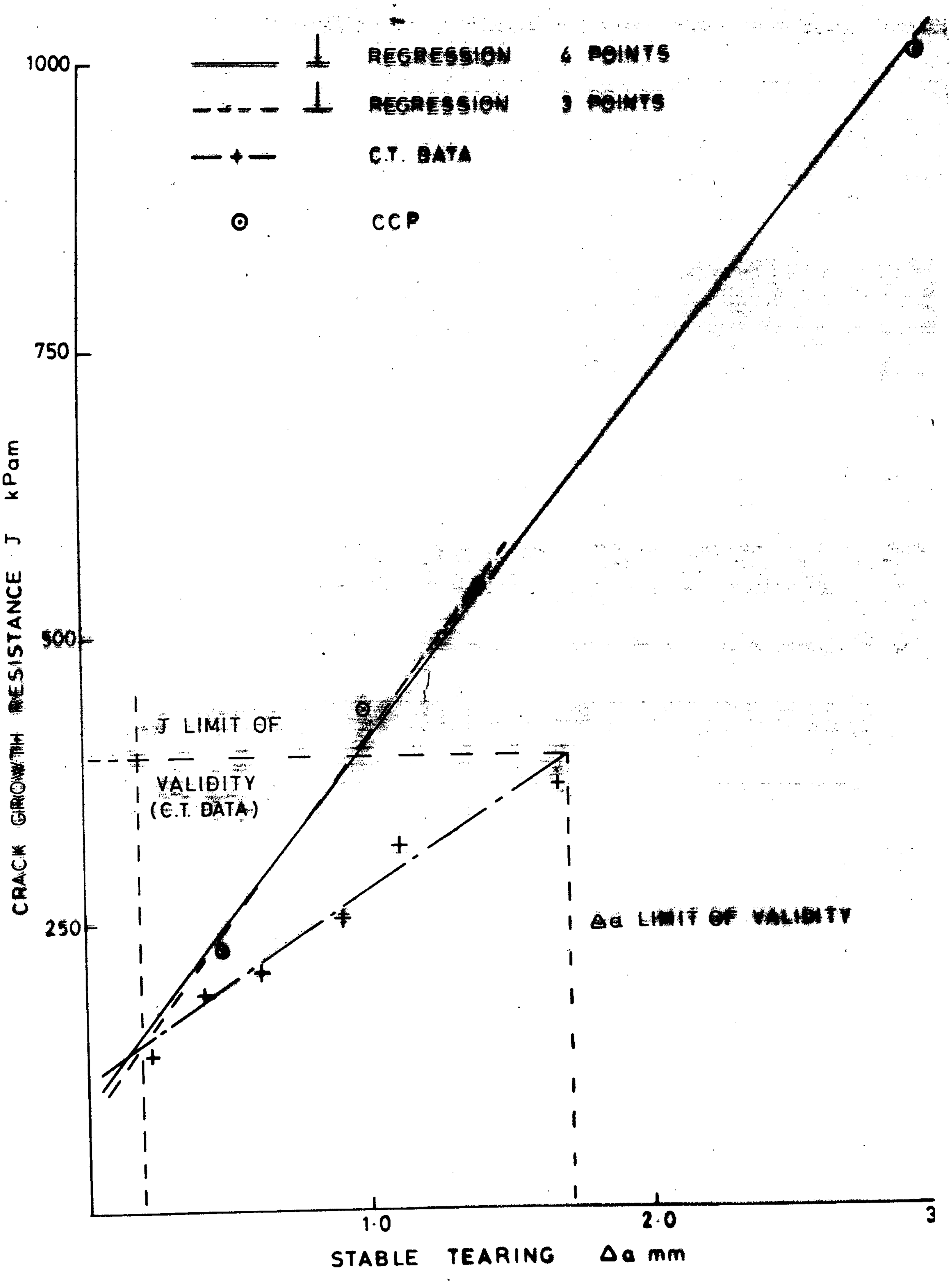

FIGURE 23 CRACK GROWTH RESISTANCE DATA FOR CARBON MANGANESE STEEL

FIG. 24 The Double Punch Specimen

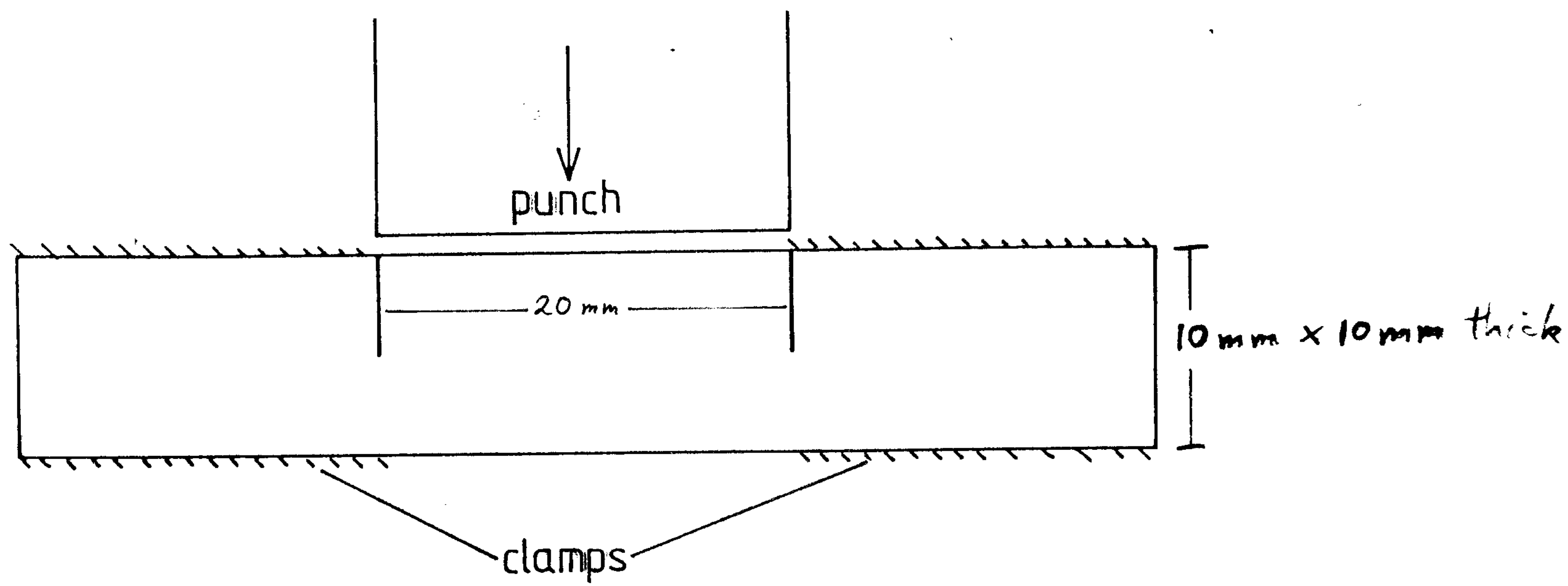

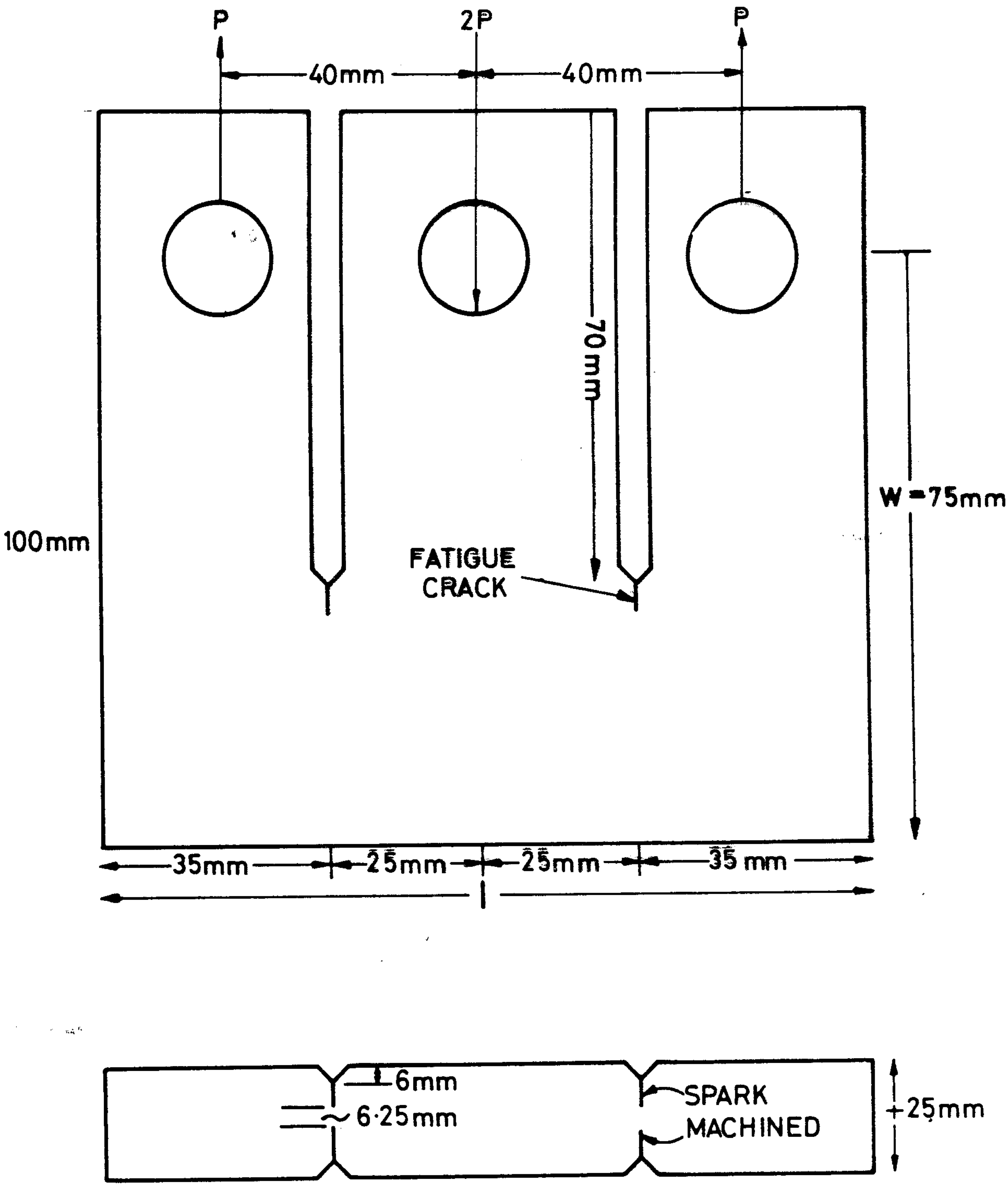

FIG. 25 COMPACT DOUBLE SHEAR SPECIMEN.

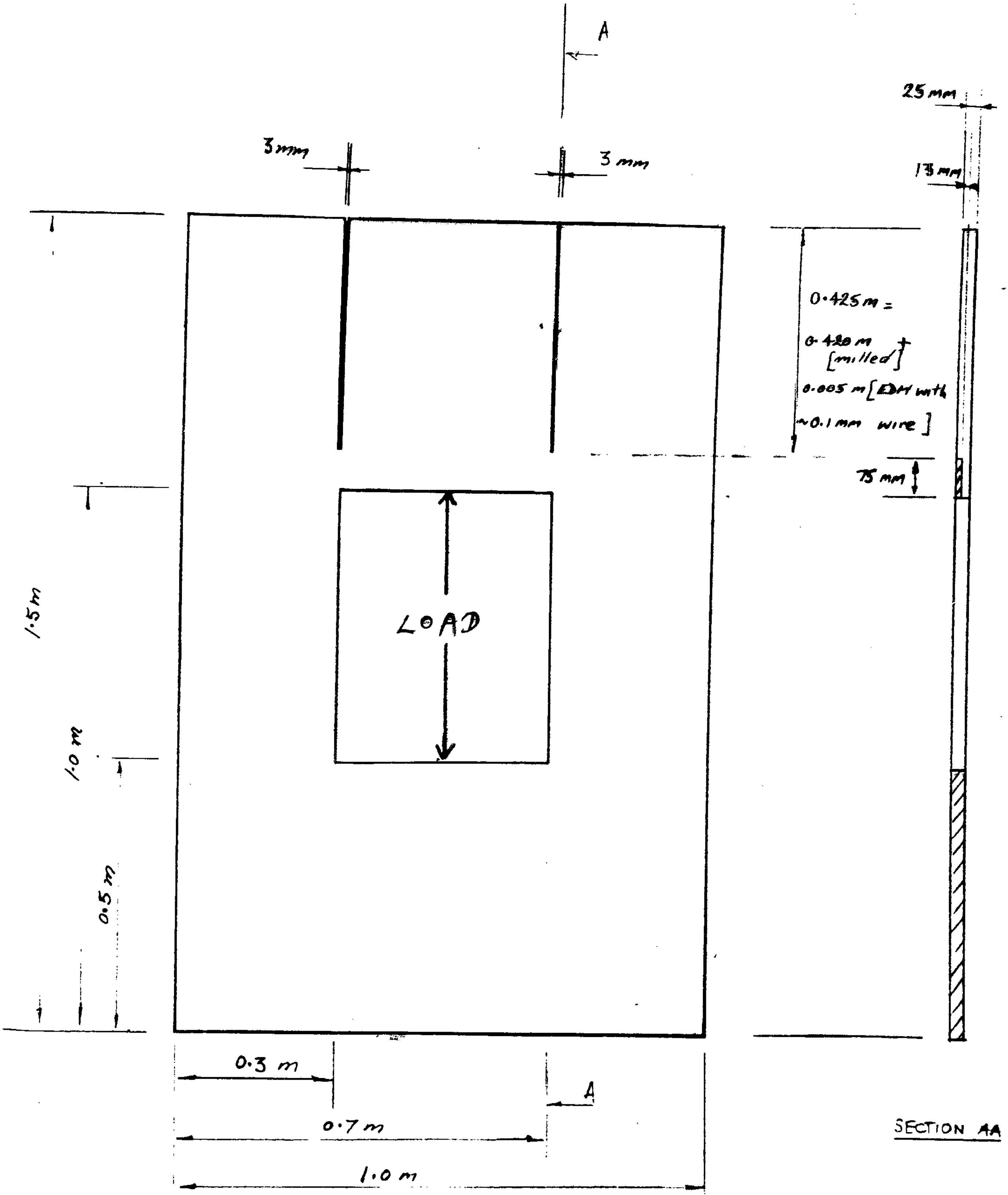

Fig 26 1st Large Shear Plate

Fig. 27 Plot of G versus U for D.P.S.

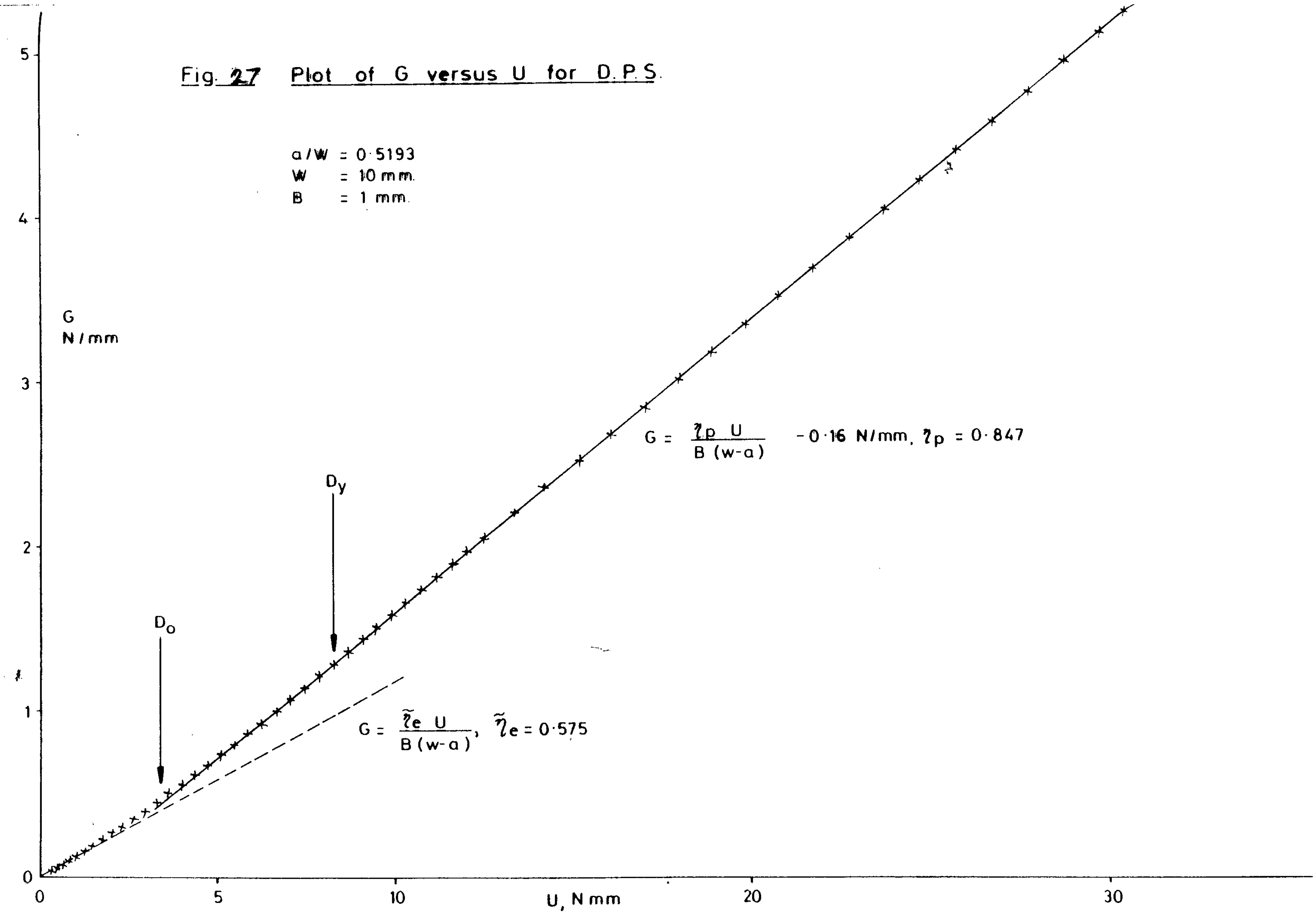

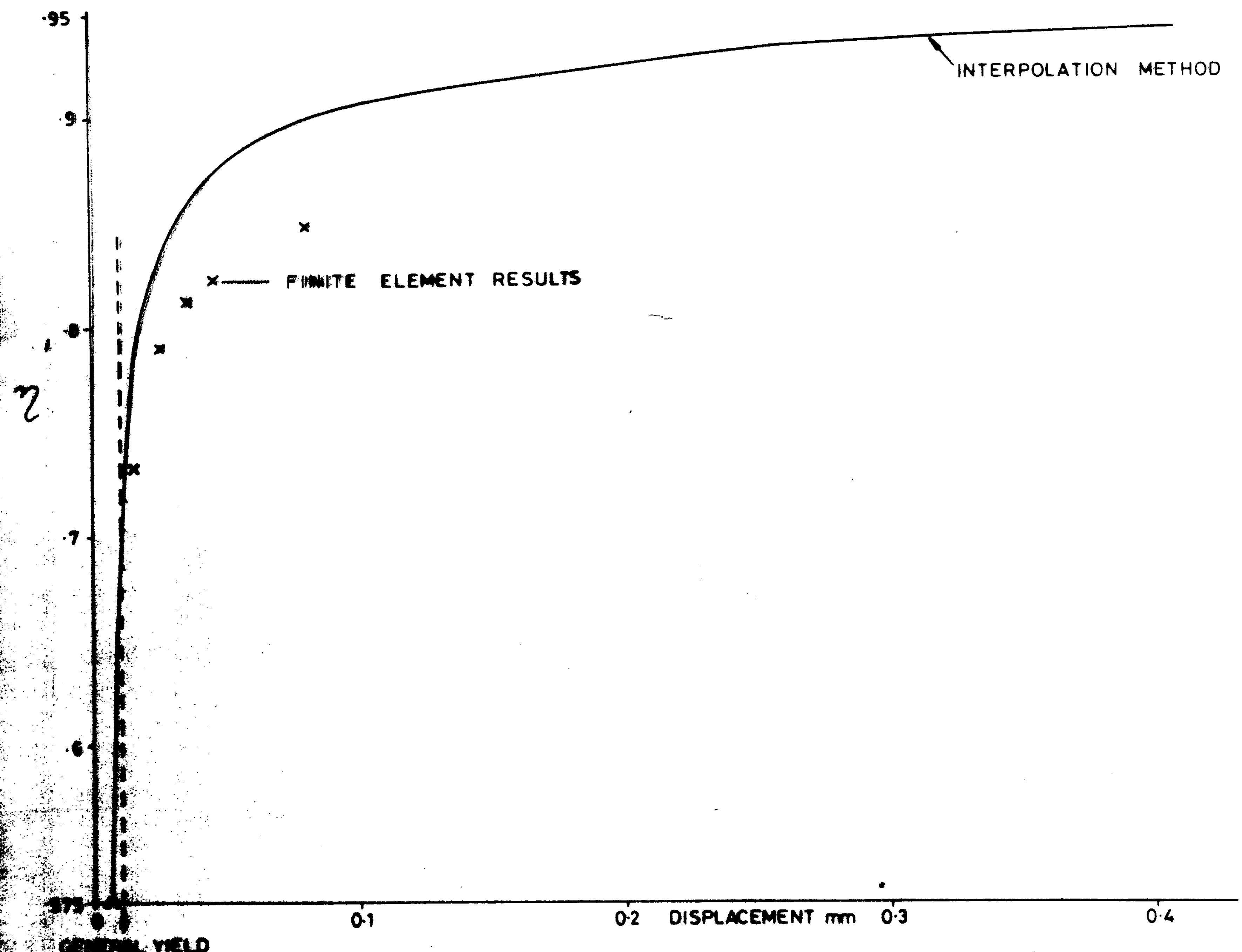

FIG. 28 FINITE ELEMENT AND INTERPOLATION METHODS OF η -EVALUATION, DPS

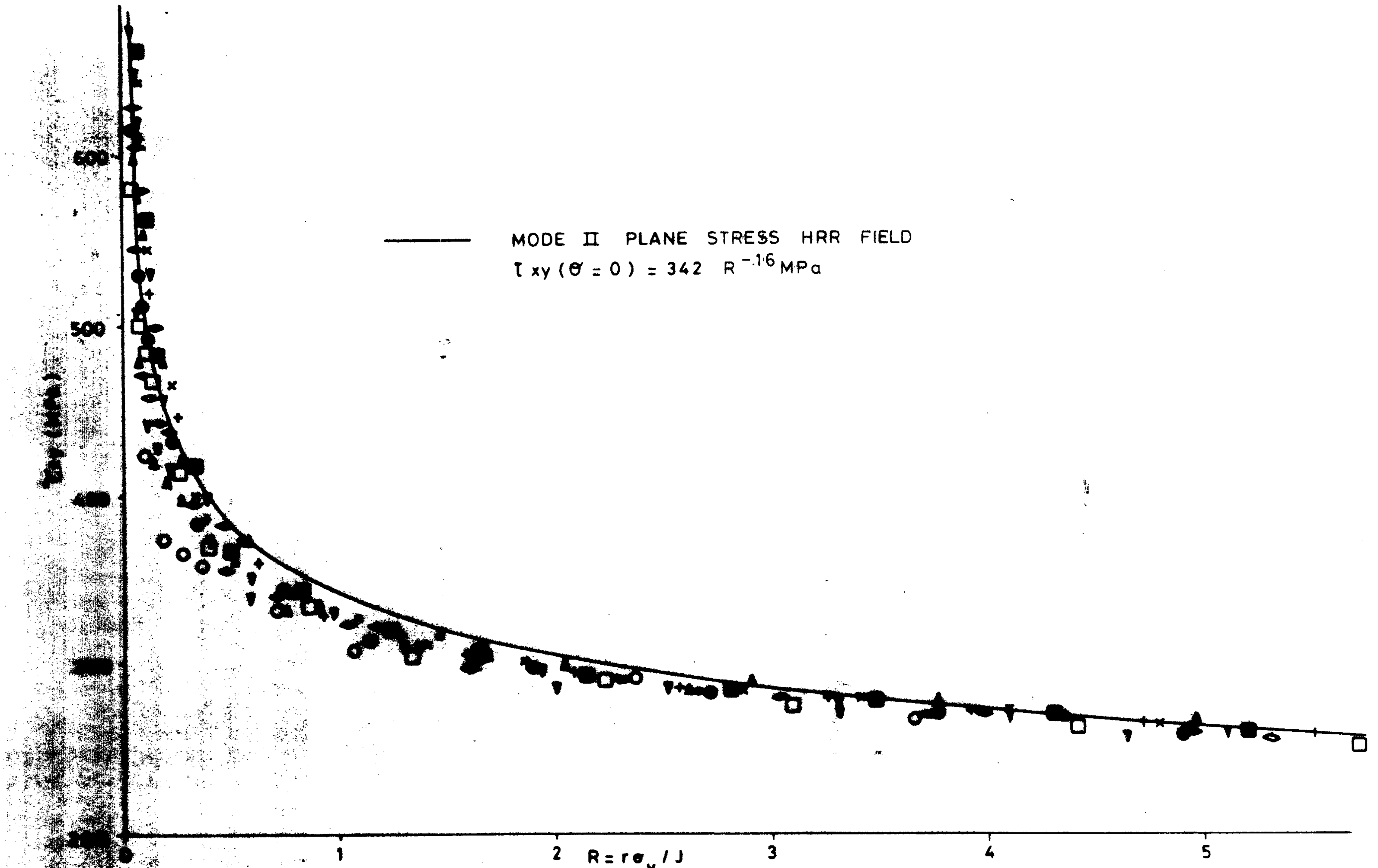

FIG. 30 SHEAR STRESS ON LIGAMENT (θ=0) VERUS NORMALIZED DISTANCE FROM CRACK TIP DPS

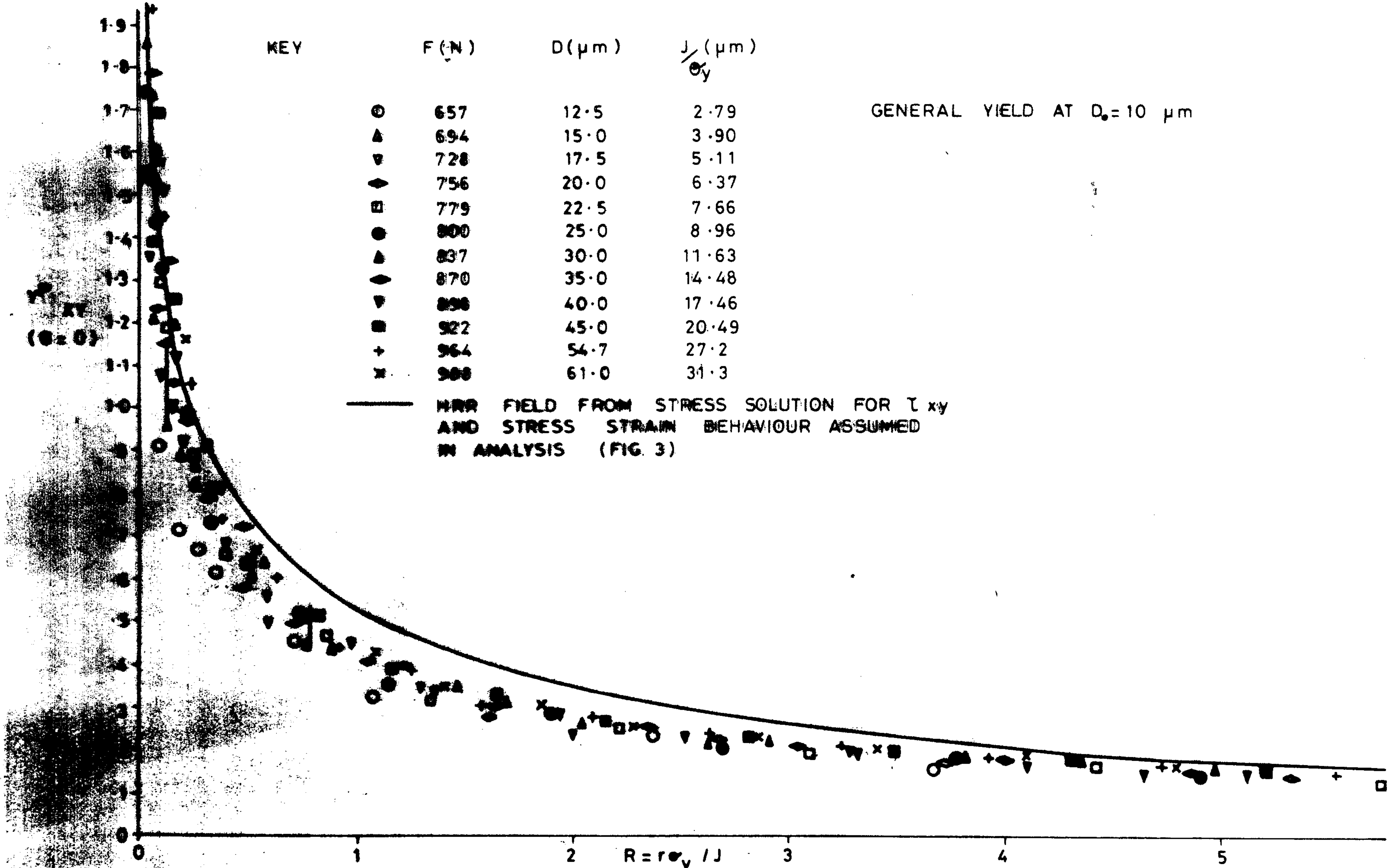

FIG. 31 PLASTIC ENGINEERING SHEAR STRAIN ON LIGAMENT ($\theta = 0$) AGAINST NORMALIZED DISTANCE FROM CRACK TIP DPS

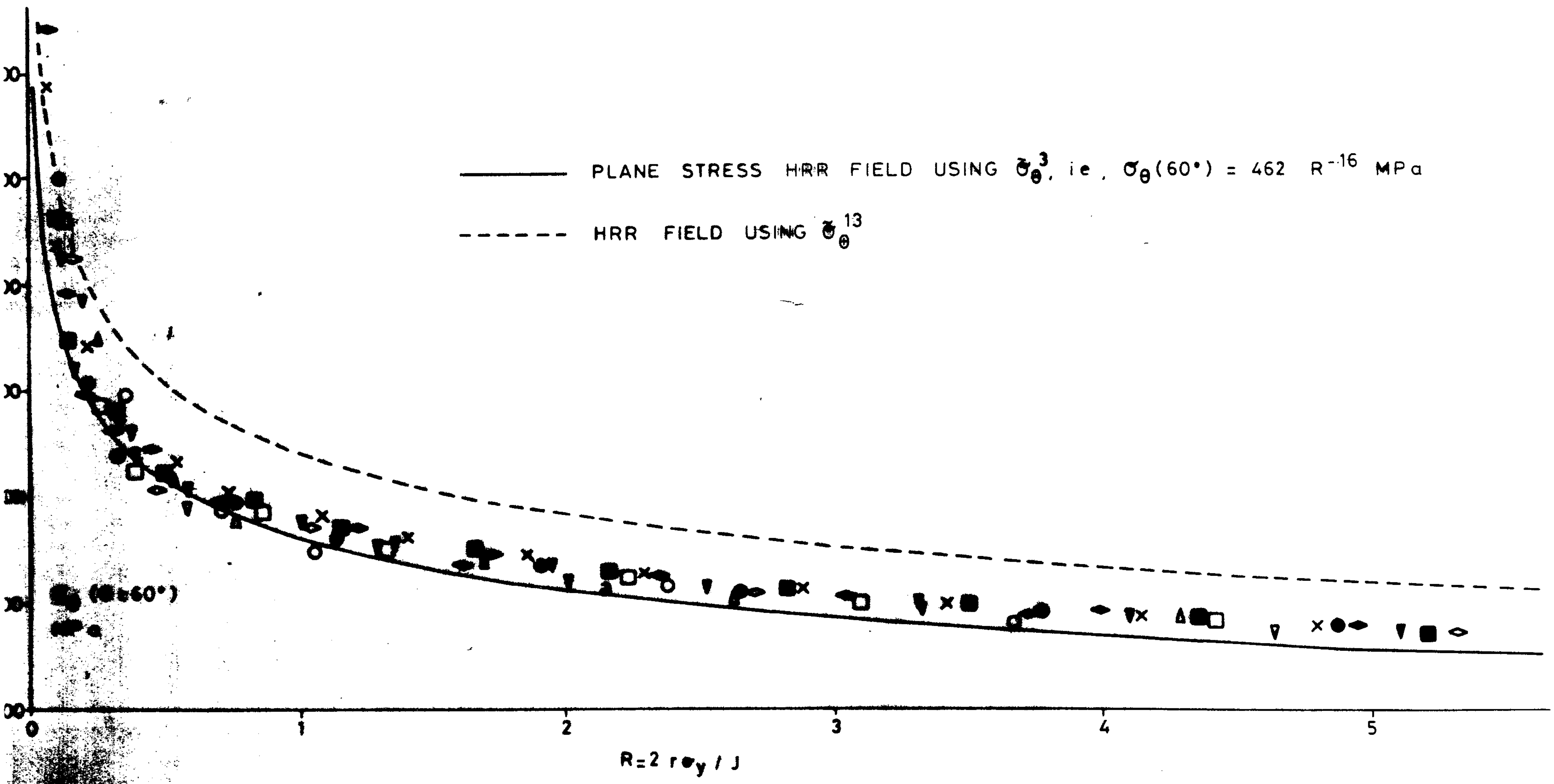

FIG. 32 θ - STRESS ON θ = 60° VERSUS NORMALIZED DISTANCE DPS

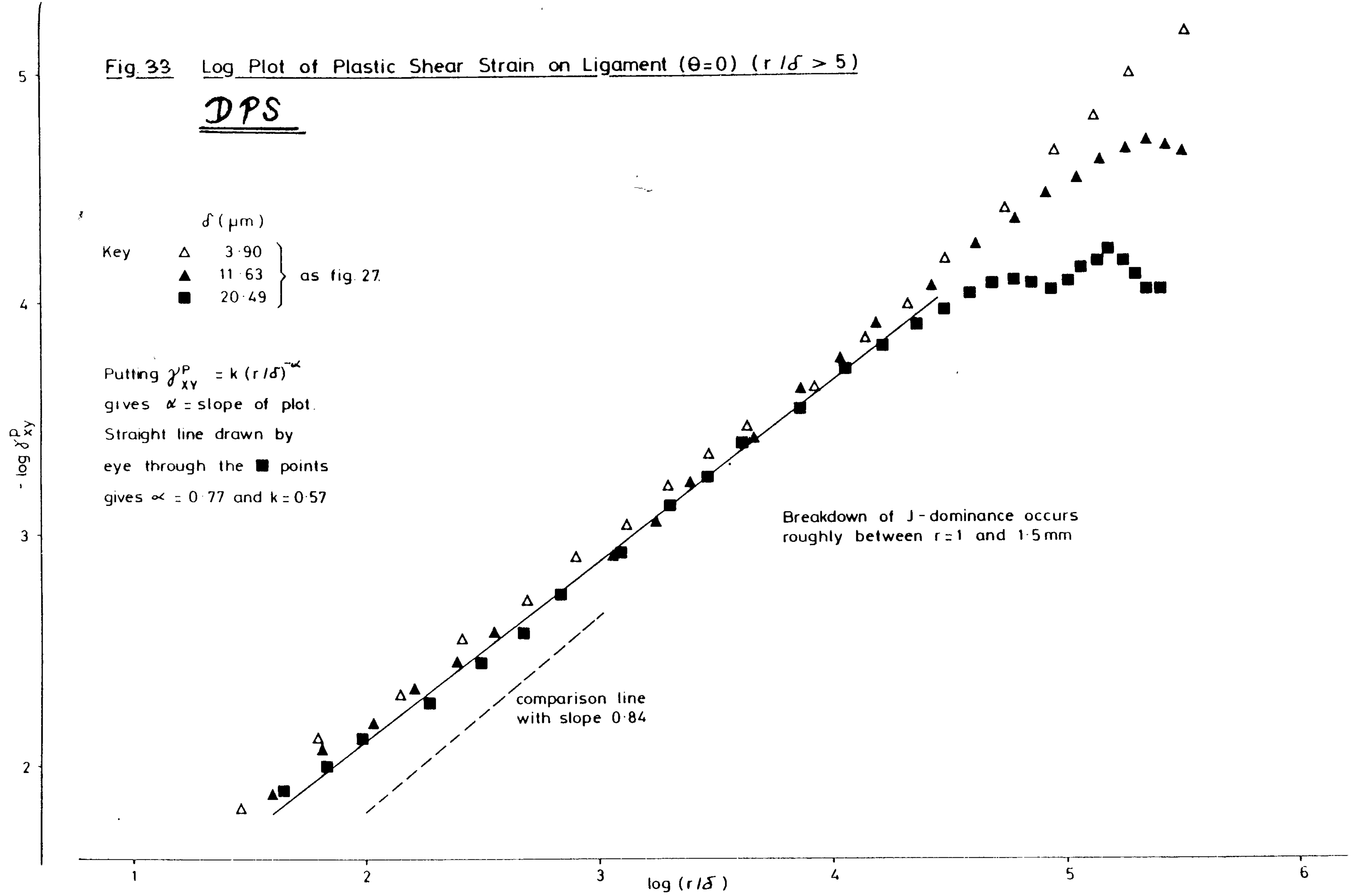

Fig. 33 Log Plot of Plastic Shear Strain on Ligament (θ=0) (r / δ > 5)

FIG. 34 COMPARISON OF CRACK GROWTH RESISTANCE CURVE FOR LARGE SIZE DPS SPECIMENS WITH STANDARD SIZE SPECIMENS.

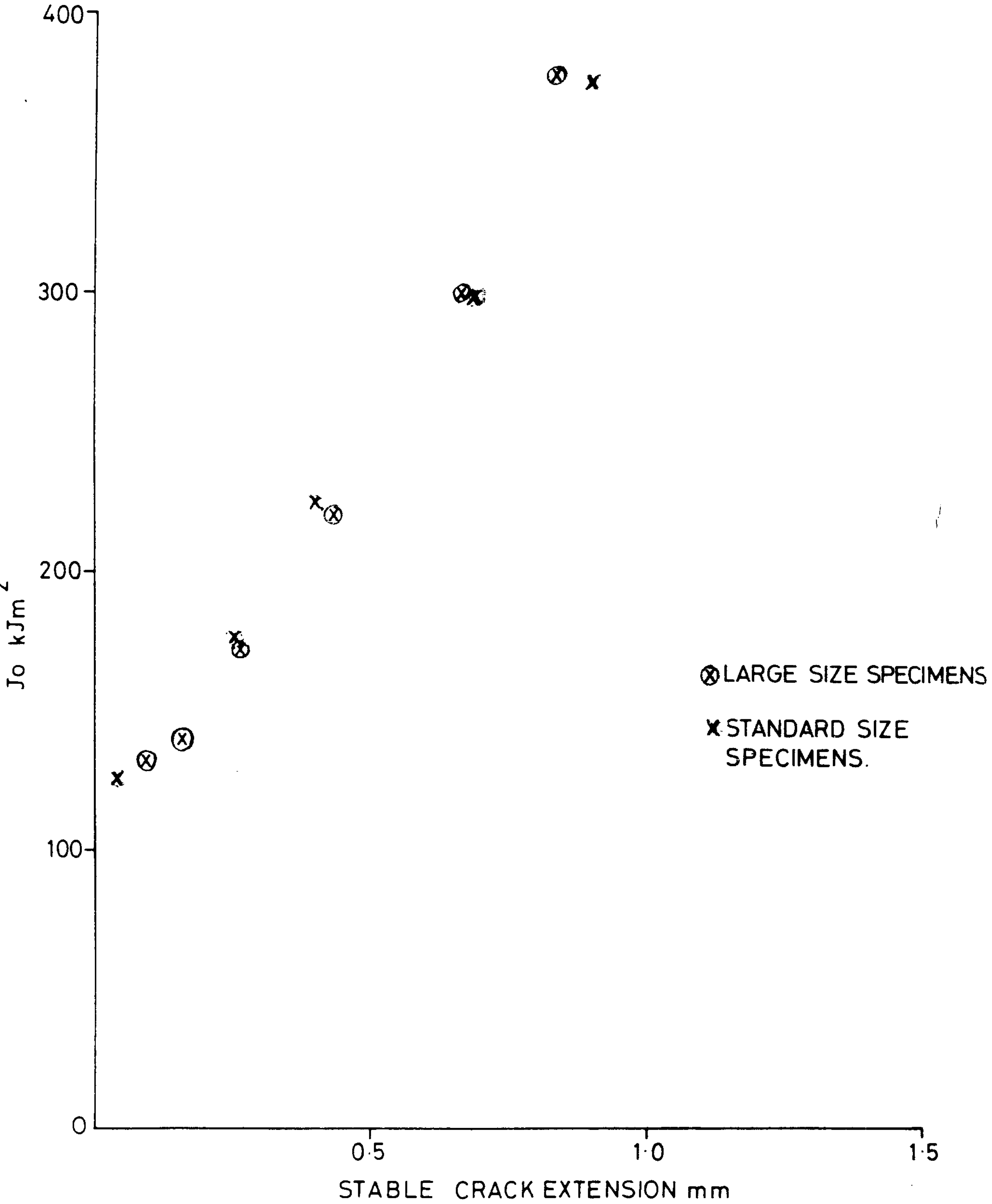

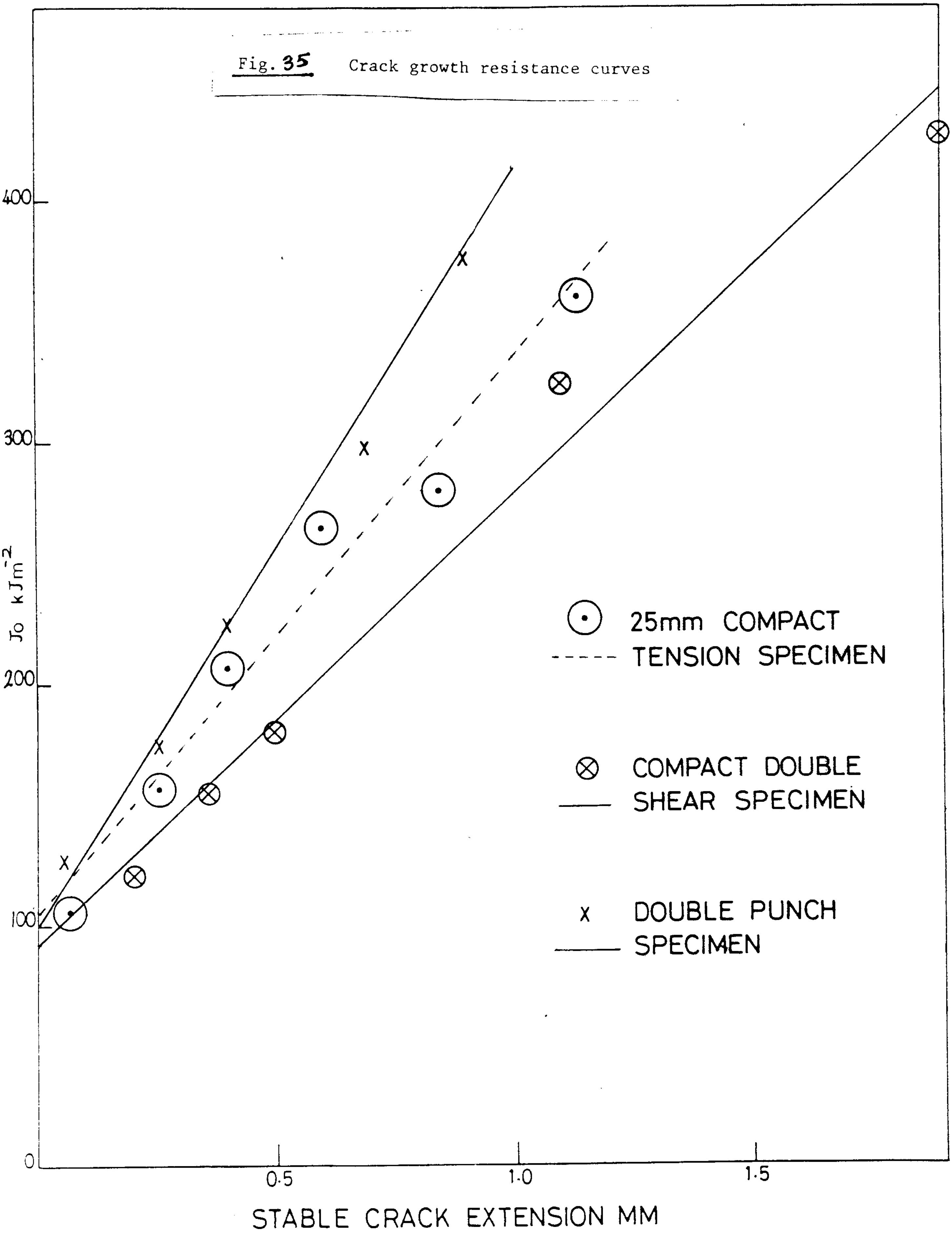
Fig. 35 Crack growth resistance curves
400
300
200
100
0
Jo kJm^{-2}
0.5
1.0
1.5
STABLE CRACK EXTENSION MM
25mm COMPACT TENSION SPECIMEN
COMPACT DOUBLE SHEAR SPECIMEN
X DOUBLE PUNCH SPECIMEN

Figure 37 Assessment Diagrams

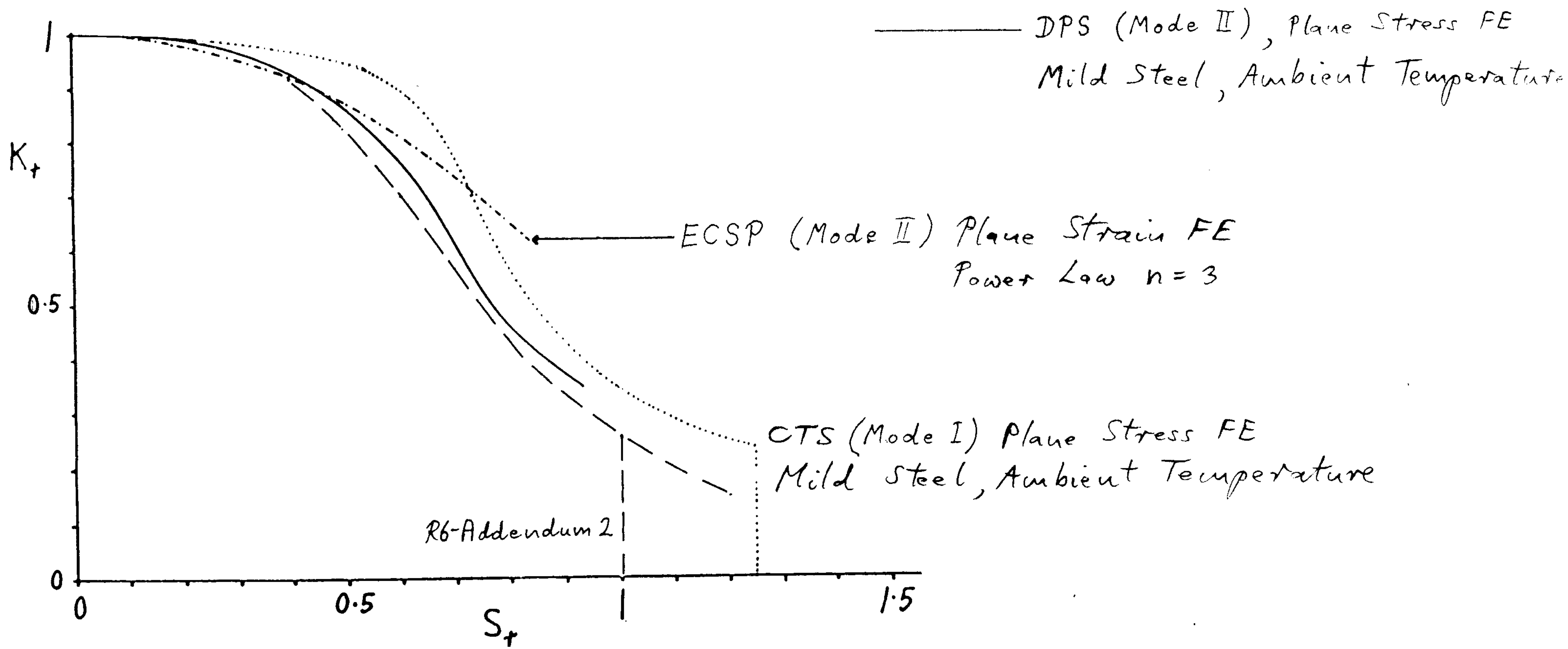

Fig. 37

MAXIMUM LOADS FOR LSS TESTS

TEST	τ_u (MPa) †	LIGAMENT* A, (MM^2)	MAX. LOAD MN (F)	$\frac{\text{MAX. LOAD}}{A \tau_u}$
1	405	73.5 x 13	.292	0.75
2	305	70 x 25	.394	0.74
3	405	199 x 7	.403	0.71

* after accounting for stable crack growth (estimated from visual observation prior to fracture in the case of Test 2).

† derived from punch specimen tests.

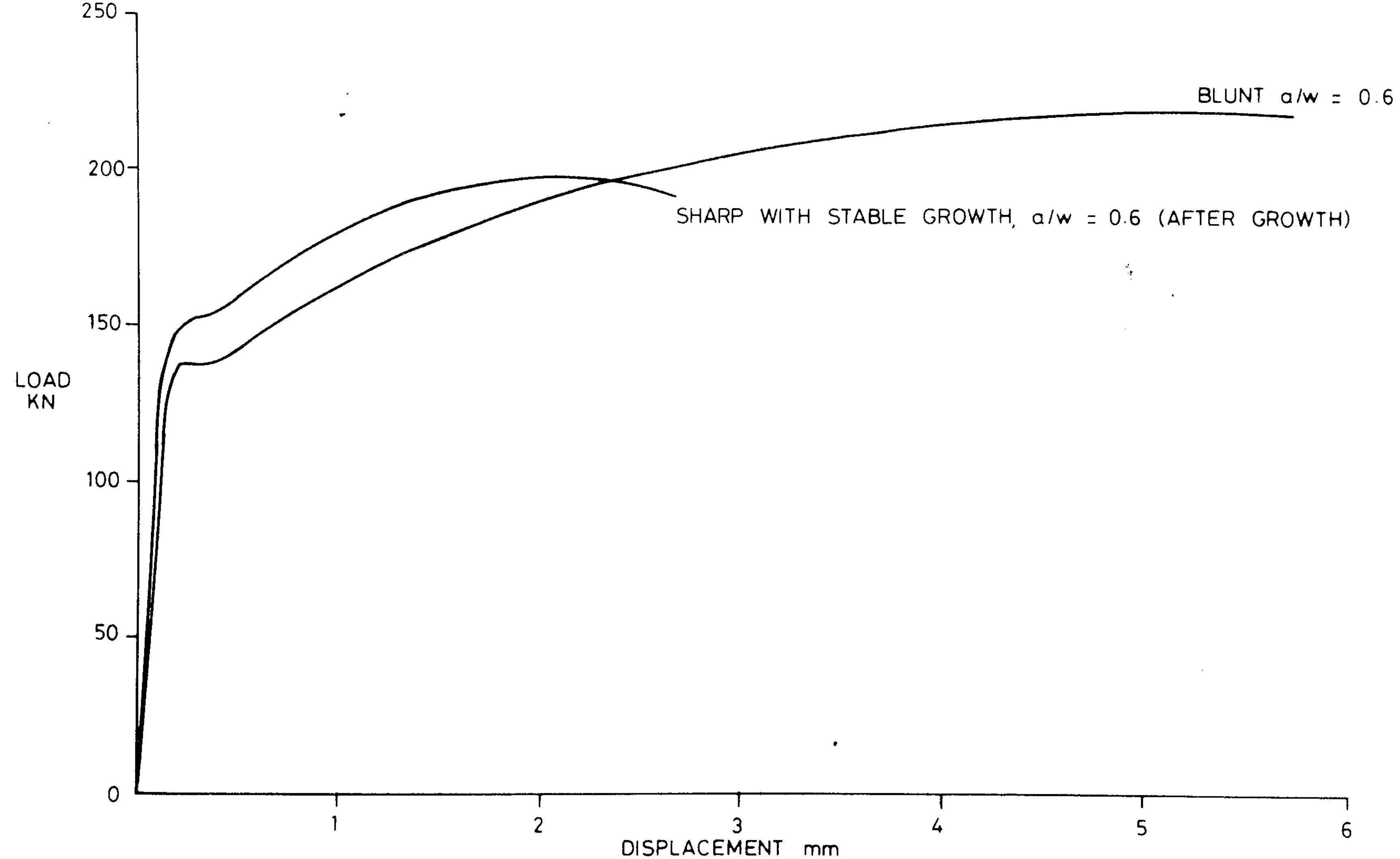

FIG. 40 COMPARISON OF LOAD/DISPLACEMENT RECORDS OBTAINED IN SHARP CRACKED AND BLUNT NOTCHED CENTRE CRACKED PANEL